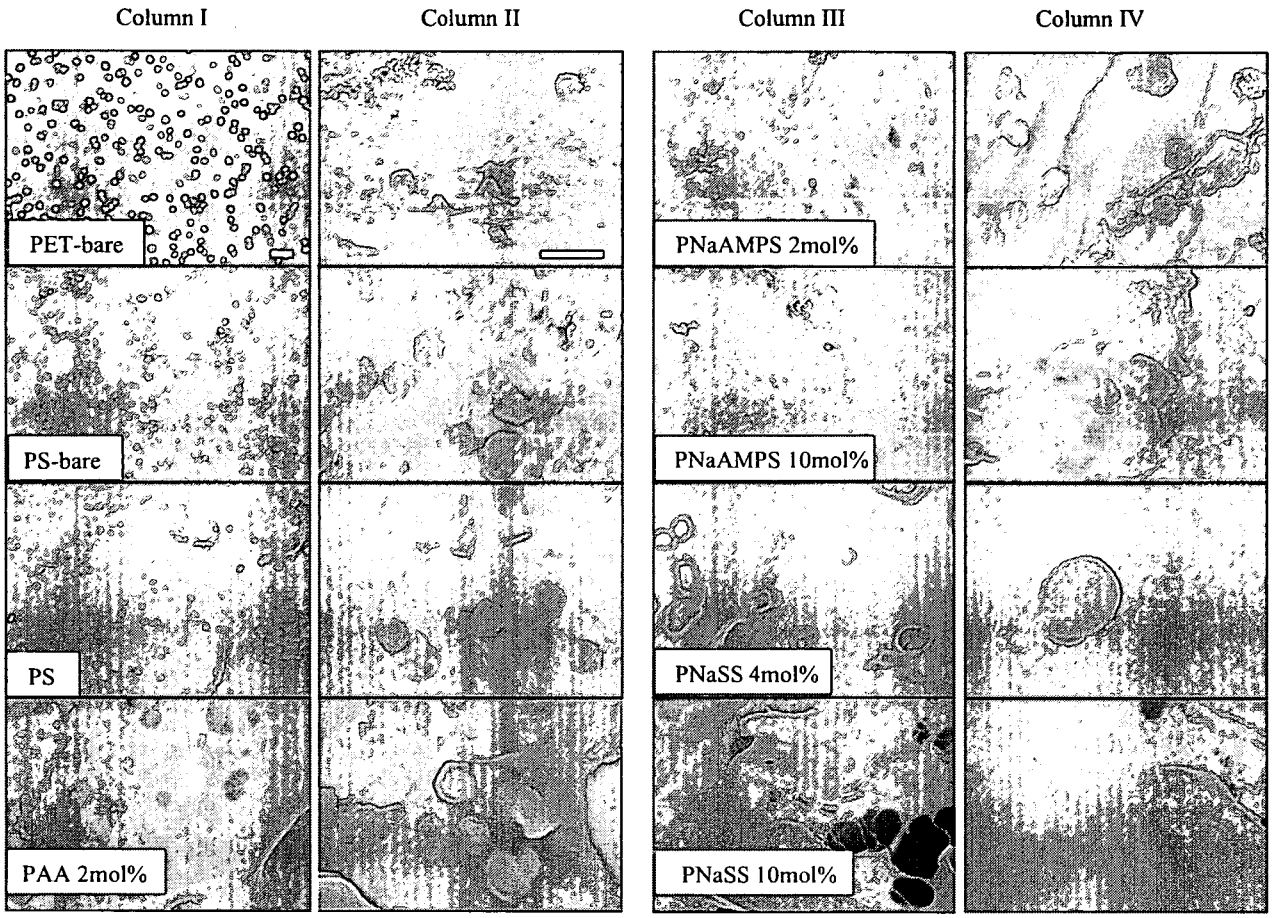

Fig. 5. SEM images of the adhered platelets on the HUVECs cultured on various kinds of substrates, and on bare PET and PS plates. The captions that have not 'bare' indicate the cultured HUVEC surface. Column II and IV is the magnified images of Column I and III, respectively. Scale bar: 5 μm.

Figs. 6 and 7 shows that by promoting the amount of HSPGs on HUVEC surface by TGF-β_1, the density of adhered platelets on the HUVECs cultured on PAA gel dramatically decreased from to 115 to 10 cells/10^4 μm^2. The density of adhered platelets on the HUVEC sheet cultured on PNaAMPS gel dramatically decreased from 183, 34 cells/10^4 μm^2 to 15, 17 cells/10^4 μm^2, respectively, for 2 and 4 mol% cross-linker concentration. The density of adhered platelets on the HUVEC sheet cultured on the 10 mol% PNaAMPS gel was 6 cells/10^4 μm^2, and it did not change by TGF-β_1 treatment. After treating the HUVECs with heparainase I that decreases the amount of the HSPGs, the density of adhered platelets on the HUVEC sheet cultured on PNaSS gel increased from 0 to 87 and 32 cells/10^4 μm^2, for 4 and 10 mol% cross-linker concentration, respectively.

We found that some platelets aggregate on the heparainase I treated HUVEC sheet cultured on 4 mol% PNaSS gel, while the adhered platelets on the as-prepared and TGF-$\beta_1$treated HUVECs are randomly distributed without aggregation (Fig. 7). Sibylle et al. reported that heparinase I induces platelets to expressed secretion maker (P-selectin) and aggregation maker (activated fibrinogen receptor GPIIb-IIIa) in vitro using whole blood flow cytometry [39]. About half of the adhered platelets aggregated on the heparainase I treated HUVEC sheet cultured on 4 mol% PNaSS gel was observed in our experiment, implying remained heparinase I on HUVEC sheet induces GPIIb-IIIa maker and further resulted to platelet aggregation. The effect of heparinase I on platelet aggregation and morphology in static conditions will be investigated in a future study.

The results show that for the cultured HUVECs that showed a large amount of platelets adhesion, after they were treated by TGF-β_1, platelet adhesion obviously decreased comparing with the as-prepared HUVECs. On the other hand, for the cultured HUVECs that did not induce platelet adhesion, after they were treated by heparinase I, platelets begun to adhere on the HUVECs. Therefore, the amount of glycocalyx on the cultured HUVECs modulates platelet adhesion. Our result is in agreement with the animal experiment that demonstrated the platelet adhesion is induced when the EC glycocalyx of vine of Golden hamsters is degraded by oxidized lipoproteins [40].

From the above results, we know that the HUVEC sheets cultured on the 4 and 10 mol% PNaSS gels, which did not induce platelet adhesion, have rich HSPGs on the cell surfaces. On the other hand, the HUVECs cultured on

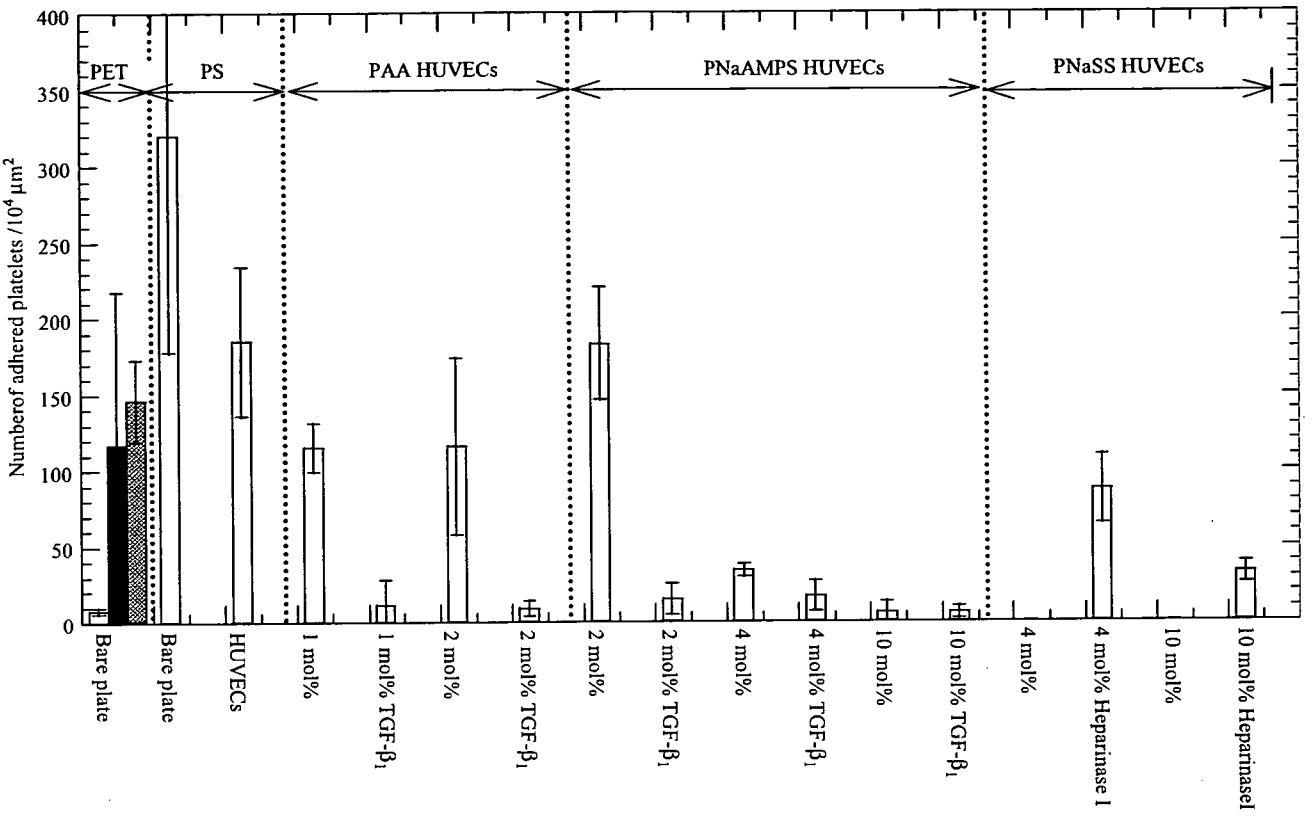

Fig. 6. Densities of adhered platelets on un-treated, TGF-β_1 treated, and heparinase I treated HUVECs cultured on various kinds of substrates, and on bare PET and PS plates. The numbers in the figures are the concentration of MBAA in molar ratio in relative to monomer used in gelation. White bar: normal platelet with spherical shape, black bar: round platelet with pseudopode extension, white bar with oblique lines: spreading platelet. Error ranges are standard deviations over $n = 3$–5 samples.

1 and 2 mol% PAA gels and 2 mol% PNaAMPS gels, which promoted a large amount of platelet adhesion, have poor HSPGs on the cell surfaces.

HajMohammadi et al. [41] reported that despite the reduction in heparin sulfate activity, the knockout mice failed to show accelerated thrombosis in the injured arteries compared with the wild-type counterparts. This finding raises the possibility that other glycosaminoglycans relate to platelet adhesion. Here, we have demonstrated that HSPGs are involve in platelet adhesion, but we do not exclude the possibility that other components of the glycocalyx, such as hyaluronic acid and chondroitin sulfate, influence platelet adhesion.

Our previous studies [42–44] showed that the freezing bound water in polymer is critical for inhibiting platelet adhesion. It suggested that sufficient amount of freezing bound water (a kind of crystallization water) prevents the blood components from direct contacting the polymer surface, which contributes to the excellent platelet compatibility. Some well-known biomaterials or polysaccharides [45–48], such as poly(ethylene glycol), gelatin, chitosan, and hyaluronic acid have freezing bound water. Our study suggested that HSPGs on the EC surface have crystallized water and the amount of crystallized water influences the blood compatibility of ECs. More detailed investigation about the state of water in glycocalyx will be undertaken in a separated study.

4. Conclusions

HUVECs can proliferate to sub-confluent or confluent on the negatively charged gels. However, not all the HUVECs cultured on the artificial scaffolds have platelet inhibition function even if they show the similar proliferation behavior. The study discoveres, for the first time to the authors' knowledge, that the HUVECs cultured on the PNaAMPS and PNaSS gels show excellent platelet compatibility, especially on the PNaSS gels. Furthermore, the platelet compatibility was enhanced when the HUVECs were treated with TGF-β_1, which stimulates synthesis of HSPGs on HUVECs surface, whereas the platelet compatibility was decreased when the HUVECs were treated with heparinase I, which disrupt HSPGs. These results indicate that the different platelet adhesion properties are attributed to the amount of glycocalyx on the HUVECs cultured on different kinds of gel scaffolds. These results demonstrate that it is possible to fabricate hybrid artificial blood vessel with high blood compatibility from PNaAMPS and PNaSS gels with ECs monolayer on their inner surfaces.

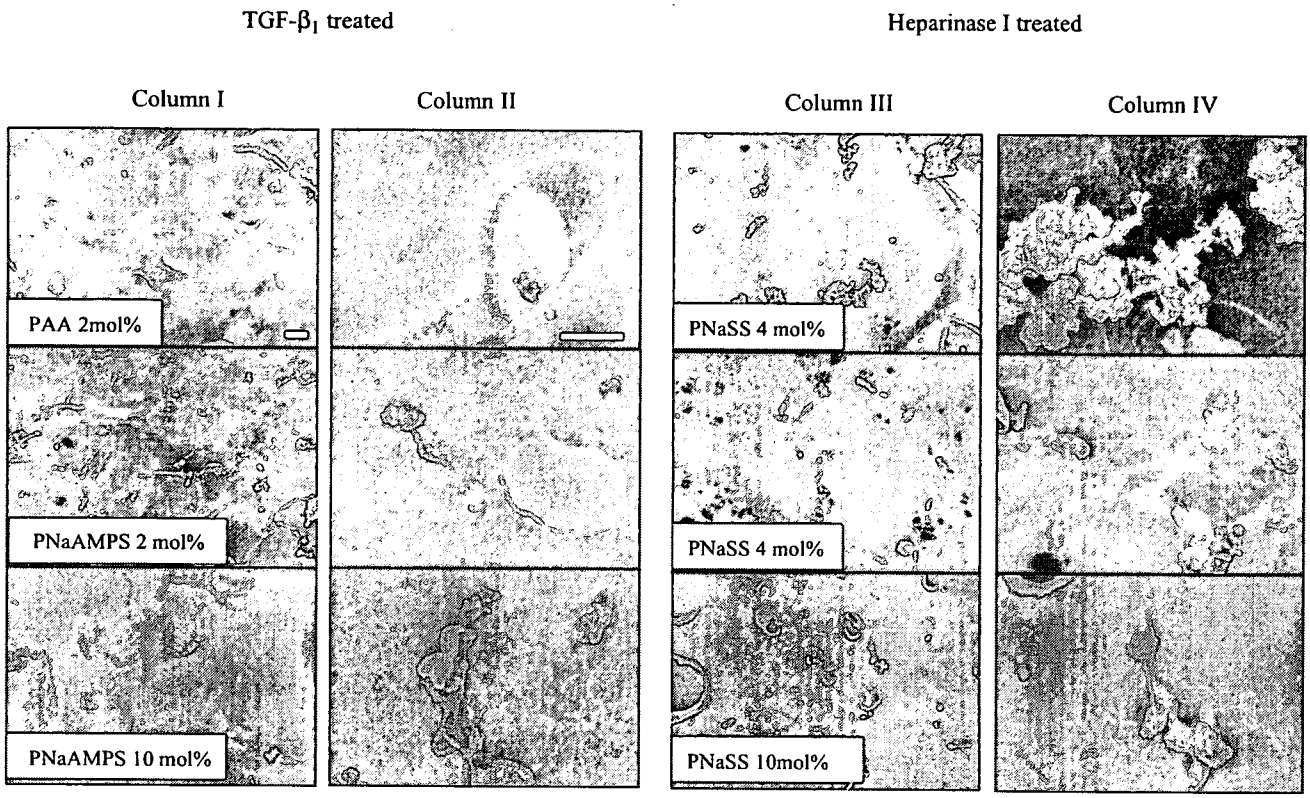

Fig. 7. SEM images of the adhered platelets on the HUVECs cultured on various kinds of gels treated by TGF-β_1 or heparinase I. Column II and IV is the magnified images of Column I and III, respectively. Scale bar: 5 μm.

References

[1] Foley DP, Melkert R, Serruys PW. Influence of coronary vessel size on renarrowing process and late angiographic outcome after successful balloon angioplasty. Circulation 1994;90(3):1239–51.

[2] Harris JM. Poly(ethylene glycol) chemistry, biotechnical and biomedical applications. New York: Plenum Press; 1992.

[3] Tanaka M, Motomura T, Kawada M, Anzai T, Kasori Y, Shiroya T, et al. Blood compatible aspects of poly(2-methoxyethylacrylate) (PMEA)—relationship between protein adsorption and platelet adhesion on PMEA surface. Biomaterials 2000;21:1471–81.

[4] Tanaka M, Motomura T, Kawada M, Anzai T, Kasori Y, Shimura K, et al. A new bloodcompatible surface prepared by poly(2-methoxyethylacrylate) (PMEA) coating—protein adsorption on PMEA surface. Jpn J Artif Organs 2000;29:209–16.

[5] Tsuruta T. Contemporary topics in polymeric materials for biomedical applications. Adv Polym Sci 1996;126:1–51.

[6] Severian D. Polymeric biomaterials. New York: Mercel Dekker, Inc.; 2002.

[7] Okano T, Nishiyama S, Shinohara I, Akaike T, Sakurai Y, Kataoka K, et al. Effect of hydrophilic and hydrophobic microdomains on mode of interaction between block copolymer and blob platelets. J Biomed Mater Res 1981;15:393–403.

[8] Losia P, Lombardib S, Brigantia E, Soldania G. Luminal surface microgeometry affects platelet adhesion in small-diameter synthetic grafts. Biomaterials 2004;25:4447–55.

[9] Brinkman E, Foot A, Does L, Bantjes A. Platelet deposition studies on copolyether urethanes modified with poly(ethylene oxide). Biomaterials 1990;3:200–5.

[10] Mori Y, Nagaoka S, Takiguchi T, Kikuchi T, Noguchi N, Tanzawa H, et al. A new antithrombogenic material with long polyethylene oxide chain. Trans Am Soc Artif Intern Organs 1982;28: 459–63.

[11] Haimovich H, Difazio L, Katz D, Zhang L, Greco RS, Dror Y, et al. A new method for membrane construction on ePTFE vascular grafts: effect on surface morphology and platelet adhesion. J Appl Polymer Sci 1997;63:1393–400.

[12] Lee JH, Khang G, Lee JW, Lee HB. Platelet adhesion onto chargeable functional group gradient surfaces. Int J Biol Macromol 2003;32:17–22.

[13] Park JH, Park KD, Bae YH. PDMS-based polyurethanes with MPEG grafts: synthesis, characterization and platelet adhesion study. Biomaterials 1999;20:943–53.

[14] Zhang J, Yuana J, Yuan Y, Zang X, Shena J, Lin S. Platelet adhesive resistance of segmented polyurethane film surface grafted with vinyl benzyl sulfo monomer of ammonium zwitterions. Biomaterials 2003; 24:4223–31.

[15] Fujimoto K, Tadokoro H, Ueda Y, Ikada Y. Polyurethane surface modification by graft polymerization of acrylamide for reduced protein adsorption and platelet adhesion. Biomaterials 1993;14:442–8.

[16] Van den Beng B, Vink H, Spaan JA. The endothelial glycocalyx protects against myocardial edema. Circ Res 2003;92:592–4.

[17] Yanagishita M, Hascall VC. Cell surface heparan sulfate proteoglycans. J Biol Chem 1992;267:9451–4.

[18] Hallgren J, Spillmann D, Pejler G. Structural requirements and mechanism for heparin-induced activation of a recombinant mouse mast cell tryptase, mouse mast cell protease-6. J Biol Chem 2001;276: 42774–81.

[19] Weitz JI. Heparan sulfate: antithrombic or not? J Clin Invest 2003; 111:952–4.

[20] Nugent MA, Nugent HM, Iozzoi RV, Sanchack K, Edelman ER. Perlecan is required to inhibit thrombosis after deep vascular injury and contributes to endothelialcell-mediated inhibition of intimal hyperplasia. PNAS 2000;97:6722–7.

[21] Segev A, Nili N, Strauss BH. The role of perlecan in arterial injury and angiogenesis. Cardiovasc Res 2004;63:603–10.

[22] Guyton JR, Rosenberg RD, Clowes AW, Karnovsky MJ. Inhibition of rate arterial smooth muscle cell proliferation by heparin. In vivo studies with anticoagulant and nonanticoagulant heparin. Circ Res 1980;46:625–34.

[23] Kaji T, Yamada A, Miyajima S, Yamamoto C, Fujiwara Y, Wight TN, et al. Cell density-dependent regulation of proteoglycan synthesis by transforming growth factor-β_1 in cultured bovine aortic endothelial cells. J Biol Chem 2000;275:1463–70.

[24] Pries AR, Secomb TW, Jacobs H. Microvascular blood flow resistance: role of endothelial surface layer. Am J Physiol 1997;273: H2272–9.

[25] Woodsa AM, Rodenberga EJ, Hilesb MC, Pavalkoa FM. Improved biocompatibility of small intestinal submucosa (SIS) following conditioning by human endothelial cells. Biomaterials 2004;25:515–5.

[26] Chen YM, Tanaka M, Gong JP, Yasuda K, Yamamoto S, Shimomura M, et al. Biomaterials used for artificial blood vessels. JP Patent no.2006-141838

[27] Lee KY, Mooney DJ. Hydrogels for tissue engineering. Chem Rev 2001;10:1869–79.

[28] Hoffman AS. Hydrogels for biomedical applications. Adv Drug Del Rev 2002;54:3–12.

[29] Chen YM, Shiraishi N, Satokawa H, Kakugo A, Narita T, Gong JP, et al. Cultivation of endothelial cells on adhesive protein-free synthetic polymer gels. Biomaterials 2005;26:4588–96.

[30] Kasinath BS. Glomerular EC proteoglycan regulation by TGF-β_1. Arch Biochem Biophys 1993;305:370–7.

[31] Linhardt RJ, Turnbull JE, Wang HM, Loganathan D, Gallagher JT. Examination of the substrate specificity of heparin and heparan sulfate lyases. Biochemistry 1990;29:2611–7.

[32] Florian JA, Kosky JR, Ainslie K, Pang Z, Dull RO, Tarbell JM. Heparan sulfate proteoglycan is a mechanosensor on endothelial cells. Circ Res 2003;93:e136–42.

[33] Mulivor AW, Lipowsky HH. Role of glycocalyx in leukocyte-endothelial cell adhesion. Am J Physiol Heart Circ Physiol 2002;283: H1282–91.

[34] Park JH, Bae YH. Hydrogels based on poly(ethylene oxide) and poly(tetramethylene oxide) or poly(dimethyl siloxane): synthesis, characterization, in vitro protein adsorption and platelet adhesion. Biomaterials 2002;23:1797–808.

[35] Zhu A, Chen T. Blood compatibility of surface-engineered poly (ethylene terephthalate) via *o*-carboxymethylchitosan. Coll Surf B: Biointerfaces 2006;50:120–5.

[36] Gappa-Fahlenkamp H, Lewis R S. Improved hemocompatibility of poly(ethylene terephthalate) modified with various thiol-containing groups. Biomaterials 2005;26:3479–85.

[37] Brockstedt U, Dobra K, Nurminen M, Hjerpe. Immunoreactivity to cell surface syndecans in cytoplasm and nucleus: tubulin-dependent rearrangements. Exp Cell Res 2002;274:235–45.

[38] Haldenby KA, Chappel DC, Winlove CP, Parker KH, Firth JA. Focal and region variations in the composition of glycocalyx of large vessel endothelial. J Vasc Res 1994;31:2–9.

[39] Kozek-Langenecker SA, Mohammad SF, Masaki T, Kamerath C, Cheung AK. The effects of heparin, protamine, and heparinase I on platelets in vitro using whole blood flow cytometry. Anesth Analg 2000;90:808–12.

[40] Vink H, Constantinescu AA, Spaan JAE. Oxidize lipoproteins degrade the endothelial surface layer implications for platelet-endothelial cell adhesion. Circulation 2000;101:1500–2.

[41] HajMohammadi S, Enjyoji K, Princivalle M, Christi P, Lech M, Beeler D, et al. Normal levels of anticoagulant heparan sulfate are not essential for normal hemostasis. J Clin Invest 2003;111:989–99.

[42] Tanaka M, Mochizuki A. Effect of water structure on blood compatibility—thermal analysis of water in poly(meth)acrylate. J Biomed Mater Res 2004;68A:684–95.

[43] Tanaka M, Mochizuki A, Ishii N, Motomura T, Hatakeyama T. Study of blood compatibility with poly(2-methoxyethyl acrylate). Relationship between water structure and platelet compatibility in poly(2-methoxyethyl acrylate-*co*-2-hyydroxyethylmeth acrylate). Biomacromolecules 2002;3:36–41.

[44] Tanak M, Motomura T, Ishii N, Shimura K, Onishi M, Mochizuki A, et al. Cold crystallization of water in hydrated poly(2-methoxyethyl acrylate) (PMEA). Polym Int 2000;49:1709–13.

[45] Hatakeyama H, Hatakeyama T. Interaction between water and hydrophilic polymers. Thermochim Acta 1995;308:3–22.

[46] Graham NB, Zulfiqar M, Nwachuku NE, Rashid A. Interaction of poly(ethylene oxide) with solvents: 2. Water-poly(ethylene glycol). Polymer 1989;30:528–33.

[47] Ratto J, Hatakeyama T, Blumstein RB. Differential scanning calorimetry investigation of phase transitions in water/chitosan systems. Polymer 1995;36:2915–9.

[48] Nishinari K, Watase M, Hatakeyama T. Effects of polyols and sugars on the structure of water in concentrated gelatin gels as studied by low temperature differential scanning calorimetry. Coll Polym Sci 1997;275:1078–82.

Available online at www.sciencedirect.com
ScienceDirect
Colloids and Surfaces A: Physicochem. Eng. Aspects 313–314 (2008) 515–519
COLLOIDS AND SURFACES A
www.elsevier.com/locate/colsurfa

Formation of hydroxyapatite on a self-organized 3D honeycomb-patterned biodegradable polymer film

Masaru Tanaka[a,b,*], Keiko Yoshizawa[c], Akinori Tsuruma[a], Hiroshi Sunami[d], Sadaaki Yamamoto[b,d], Masatsugu Shimomura[a,b]

[a] *Nanotechnology Research Center, Research Institute for Electronic Science, Hokkaido University, Kita-Ku N21W10, Sapporo 001-0021, Japan*
[b] *CREST, Japan Science and Technology Agency (JST), Honchou 4-1-8, Kawaguchi 332-0012, Japan*
[c] *Graduate School of Science, Hokkaido University, Kita-Ku N8W10, Sapporo 060-0810, Japan*
[d] *Creative Research Initiative "Sousei", Hokkaido University, Kita-Ku N21W10, Sapporo 001-0021, Japan*

Received 29 November 2006; accepted 1 May 2007
Available online 9 June 2007

Abstract

The design of nano- and microstructures based on self-organization is a key area of research in the search for new biomaterials, and such structures have a variety of potential applications in tissue engineering scaffolds. We have reported a honeycomb-patterned polymer film (honeycomb film) with highly regular pores that is formed by self-organization. In order to utilize the honeycomb film as a scaffold for bone tissue engineering, hydroxyapatite (HA) was formed on the honeycomb film. In this study, we prepared a 3D scaffold comprising HA and a poly(ε-caprolactone) honeycomb film in a simulated body fluid (SBF) by changing the degree of hydrophilicity of the film. We investigated the dependence of the amount of HA formed on the length of time for which hydrolysis and soaking in SBF were carried out. Further, we characterized the crystallinity of the HA thus formed. We clarified that the amount of HA formed and its crystallinity were controlled by the length of time for which hydrolysis and soaking of the film were carried out. These HA-deposited honeycomb films, which have the HA microstructure, could serve as a novel scaffold for bone tissue engineering.

Keywords: Hydroxyapatite; Self-organization; Scaffold; Honeycomb; Porous

1. Introduction

Three-dimensional (3D) porous scaffolds fabricated from biodegradable polymers have been widely used as temporary extracellular matrices and play critical roles in tissue engineering. 3D scaffolds of appropriate pore size and porosities and with interconnected pores are required to facilitate cell adhesion, proliferation, differentiation, and eventual tissue regeneration in a natural manner [1–4]. A number of highly useful fabrication methods, including phase separation and lithography techniques, have been developed and applied to the fabrication of porous scaffolds from biodegradable polymers [5–8]. However, these techniques require a large amount of energy and involve many processes. In addition, a limited variety of materials is available for use as scaffolds. Each of these approaches is very different and has a unique set of characteristics that have some limitations, including uncontrolled pore size and size distribution. As a result, there is a high demand for suitable alternative methods that can be used for preparing scaffolds. Inspired by the organization of biological structures, the self-organization of organic and inorganic components into hierarchical and sophisticated structures offers an alternative to the conventional techniques of nano- and microfabrication. The process occurs under ambient physiological conditions in contrast to typical fabrication techniques that require harsh conditions. It can be applied to polymer fabrication because of its physical generality. We have found that regular structures are formed during the casting of polymer solutions on solid surfaces; for example, self-organized honeycomb-patterned films (honeycomb films) with highly regular porous

* Corresponding author. Present address: Institute of Multidisciplinary Research for Advanced Materials (IMRAM), Tohoku University, Japan. Tel.: +81 11 706 9255; fax: +81 11 706 9345.
E-mail address: tanaka@poly.es.hokudai.ac.jp (M. Tanaka).

0927-7757/$ – see front matter © 2007 Elsevier B.V. All rights reserved.
doi:10.1016/j.colsurfa.2007.05.081

structures can be prepared under humid casting conditions [9–20].

There is a growing need for hard tissue (bone, cartilage, teeth, etc.) regeneration for the treatment of various clinical diseases such as osteoporosis and arthritic disorders. However, current therapies for hard tissue diseases involve the use of autografts, allografts, and other artificial materials that are far from ideal, and each of these has its own specific problems and limitations [21]. As a result, there is a high demand for suitable alternative methods for preparing such materials. Bioactive ceramics such as hydroxyapatite (HA; $(Ca_{10}(PO_4)_6(OH)_2)$) have been widely used as hard tissue substitute materials because they can directly bond with the bone and have excellent biocompatibility [22]. In our previous studies, we found that endothelial cells [20] and neural stem cells [15] can proliferate on a honeycomb film. In order to utilize the honeycomb film as a scaffold for bone tissue engineering, hydroxyapatite (HA) was formed on the honeycomb film. In this study, we prepared HA on the honeycomb film in a simulated body fluid (SBF) by changing the degree of hydrophilicity of the honeycomb film. We investigated the dependence of the amount of HA formed on the length of time for which hydrolysis and soaking in SBF were carried out. Further, we characterized the crystallinity of the HA thus formed. This study serves as an important first step toward the development of honeycomb film-based biomimetic composite materials with enhanced tissue–implant interactions.

2. Experiment

Honeycomb films were fabricated by applying moist air to spread the polymer solution containing a biodegradable polymer (poly(ε-caprolactone): PCL) and an amphiphilic polymer (copolymer of dodecylacrylamide and ω-carboxyhexylacrylamide: Cap). PCL and Cap (10:1 wt.%) were dissolved in chloroform at a concentration of 5 g/L. The polymer solution was poured into a round glass dish (9.3 cm in diameter) with simultaneous blowing of highly humid air. Regular honeycomb structures with a pore diameter of ca. 10 μm and a wall thickness of ca. 10 μm were formed. As a reference, a flat film was prepared by a spin coater (1H-7D, Mikasa) under dry conditions. Both the flat and honeycomb films were hydrolyzed by soaking in a 1N NaOH aqueous solution (0–720 min) in order to increase the density of the hydrophilic groups. The static contact angle of the films was then measured at room temperature by the sessile drop method using a contact angle goniometer (Face CA-A, Kyowa Interface Science). The hydrolyzed honeycomb films were then soaked for 1–21 days at pH 7.4 and 37 °C in 30 ml of SBF containing different concentrations of ions (Na^+ 142.0, K^+ 5.0, Mg^{2+} 1.5, Ca^{2+} 2.5, Cl^- 148.8, HCO_3^- 4.2, HPO_4^{2-} 1.0, and SO_4^{2} 0.5 mM); these concentrations were similar to those found in human blood plasma [23–27]. SBF was prepared by dissolving reagent-grade NaCl, $NaHCO_3$, KCl, $K_2HPO_4{\cdot}3H_2O$, $MgCl_2{\cdot}6H_2O$, $CaCl_2$, and Na_2SO_4 (Nacalai Tesque Inc.) in distilled water and buffering at pH 7.4 with tris(hydroxymethyl)aminomethane ($(CH_2OH)_3CNH_3$) and 1.0 M hydrochloric acid (Nacalai Tesque Inc.) at 37 °C. The films were then removed from SBF, soaked in distilled water, and dried at room temperature. After mounting the dried samples on aluminum stages by using double-stick tape, they were coated with palladium gold (approximately 5 nm of coating) by using an ion sputter coater (E-1030, Hitachi). Subsequently, the surface morphology was observed under a scanning electron microscope (SEM; S-3500N, Hitachi). The amount of HA deposition was estimated by energy dispersive X-ray microanalysis (EDX; HD-2000, Hitachi) and X-ray diffraction (XRD; RINT2500, Rigaku). The crystallinity of HA was estimated by XRD. The surface roughness was observed under an atomic force microscope (AFM NanoScope IIIa, Veeco). The surface roughness was defined by the following equation: roughness = surface area of sample/ideal flat surface area.

3. Results and discussion

We fabricated the honeycomb films formed by a solution casting technique in humid air. The film showed a highly regular hexagonal arrangement of pores (honeycomb-patterned structure) and a well-interconnected, uniform pore structure, as shown in Fig. 1. The 3D structure could affect the flow of nutrients and wastes. Condensation of water from the air due to evaporation and cooling occurred when a water-immiscible solvent was used. Self-packed and monodispersed water droplets that formed on the solution surface acted as a temporary template for the pores. Cap acts as a surfactant and contributes to the stabilization of the water droplets at the interface of the polymer solution and water. As a result, fusion of the water droplets is prevented due to the intervening Cap layer. Most polymers dissolved in a water-immiscible solvent can be fabricated into a honeycomb film by the addition of Cap. This method has several advantages—the films can be prepared easily, at a low cost, and without any limitations pertaining to the availability of materials for the scaffold. The process is relatively easy to scale up and is being used for the commercial production of porous scaffolds.

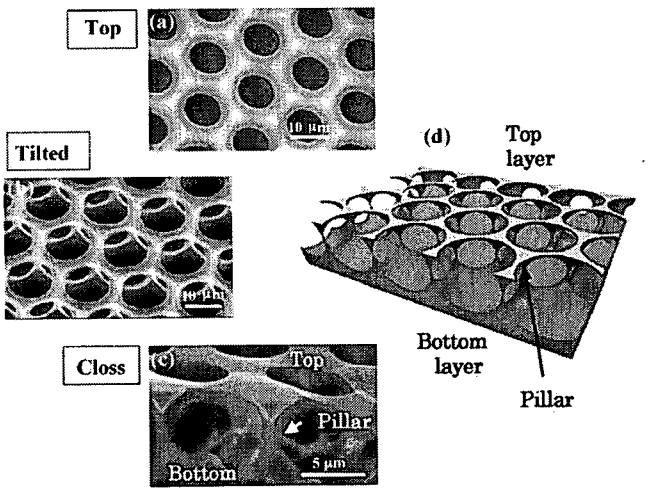

Fig. 1. SEM images of the honeycomb film in different views: (a) Surface, (b) tilted, and (c) cross-section. (d) Schematic representation of the 3D structure of the honeycomb film. The pore structure (spherical shape) reflects the behavior of the condensed water droplet as a template.

Biominerals provide a unique inspiration for material design as illustrated by Nature's ability to manipulate poor engineering materials such as HA. Biominerals are typically composite materials that are intimately associated with polymers and exhibit a hierarchical organization on the length scale that ranges from the nanometer scale to a macroscopic level. Such a "bottom-up" approach will facilitate our understanding of structure–function relationships in template-driven biomineralization and will help us in deriving a set of rules that could guide the rational design of composite materials in the future.

If honeycomb films are endowed with HA-forming ability, it will be possible to develop soft and hard tissue implants that can bond to hard and soft tissues and regenerate in a natural way. In general, HA is formed on carboxyl group-containing surfaces in SBF that has ion concentrations similar to those found in human

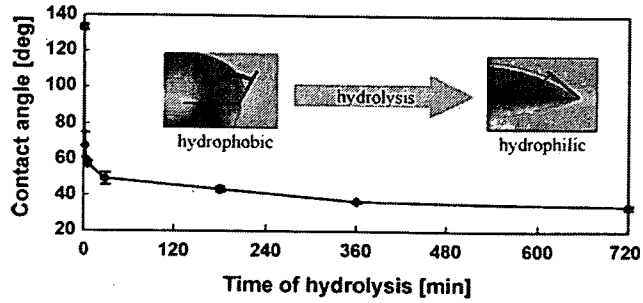

Fig. 2. Static contact angles of the honeycomb films. The films were hydrolyzed by soaking in a 1N NaOH aqueous solution (0–720 min). $n = 8$.

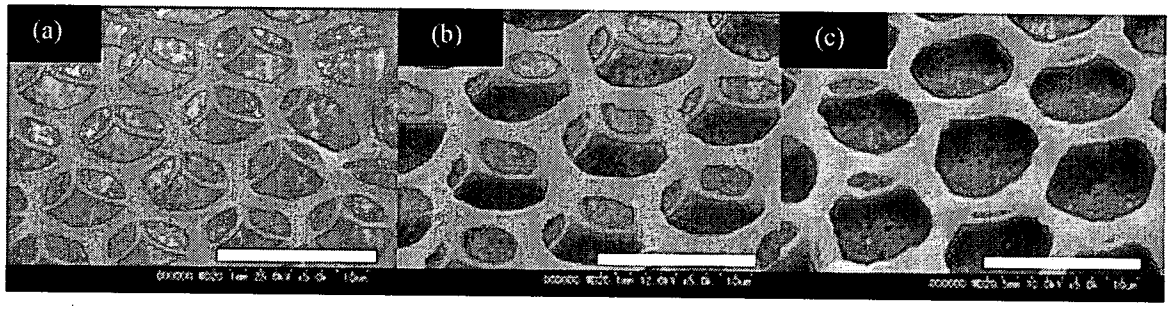

Fig. 3. SEM images (tilted angle: 50°) of the surface of honeycomb films that were first hydrolyzed for 360 min and then soaked in SBF. (a) Before soaking in SBF. (b) After soaking in SBF for 7 days. (c) After soaking in SBF for 21 days. Bar: 10 μm.

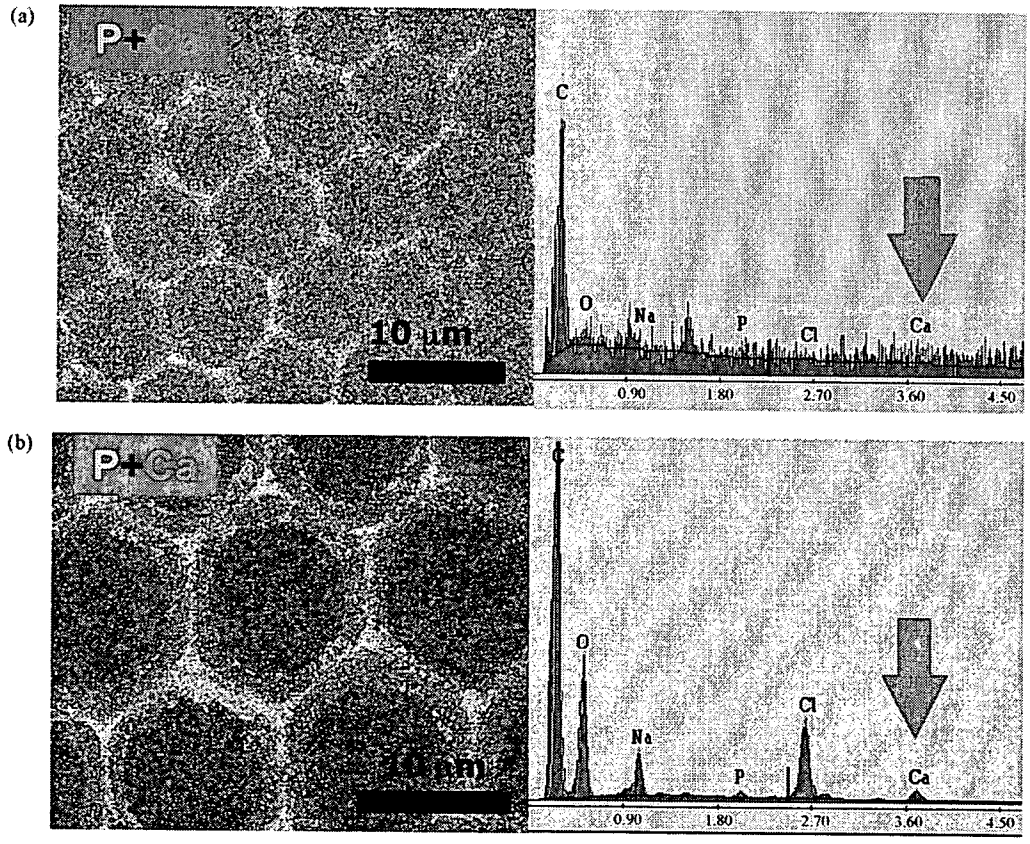

Fig. 4. EDX patterns of the honeycomb films that were first hydrolyzed for 360 min and then soaked in SBF. (a) Before soaking in SBF. (b) After soaking in SBF for 21 days.

blood plasma, which is supersaturated with respect to HA. In this study, both flat and honeycomb films were hydrolyzed by soaking in a 1N NaOH aqueous solution in order to introduce carboxyl groups on the films. Fig. 2 shows the static contact angle of the honeycomb films. The contact angle of the initial honeycomb film was approximately 130°. This indicates an increase in the hydrophobicity when compared with a flat film that has a contact angle of 110°. The contact angle of the honeycomb films gradually decreased from 130° to 40° as the time for hydrolysis was increased; this was due to the generation of oxygen-based functional groups on the film surface as a result of the partial hydrolysis of the PCL ester main chain by the NaOH aqueous solution. To obtain a better understanding of the relationship between the surface chemistry of the film and HA formation, we applied the same HA formation technique to the PCL honeycomb film. Formation of an HA layer on the honeycomb films after soaking in an SBF solution was evidenced from the following analyses: SEM, EDX, XRD, and AFM. First, changes in the surface characteristics of the honeycomb film before and after soaking in SBF were observed by SEM imaging. The SEM images showed deposits on the honeycomb film after soaking in SBF (Fig. 3b and c); such deposits were not observed prior to soaking in SBF (Fig. 3a). The EDX profiles of the honeycomb films before and after soaking in SBF are shown in Fig. 4a and b. Results of the EDX analysis show changes in elemental distribution. The appearance of phosphorus (P) and calcium (Ca) bands in the spectra on the honeycomb film after soaking in SBF was detected by EDX analysis (Fig. 4b). The Ca/P ratio of 1.6 observed for HA is approximately the same as that reported for the stoichiometric composition of HA ($Ca_{10}(PO_4)_6(OH)_2$). Further, several diffraction peaks (0 0 2, 2 1 0, 2 1 1/1 1 2, 3 0 0, 2 0 2, and 3 1 0) that are typical to HA were observed on XRD (Fig. 5). The XRD pattern of the honeycomb film soaked for 21 days is similar to that observed for synthetic or biological HA of poor crystallinity [23–28]. The sharp (0 0 2) reflection indicated the preferred orientation of the HA crystallite. Both the EDX and XRD patterns indicated that the HA deposited on the honeycomb film is composed of low crystalline defective nanocrystallites of HA that incorporate minor elements such as Na. In fact, these are the characteristics that are typically observed in the HA formed on bioactive ceramics in SBF and are similar to those of biological HA found in bone tissue [28–32]. Both the EDX and XRD patterns of the honeycomb film observed prior to soaking are also shown as references, and no peak typical to HA was observed in either of these patterns. Based on the EDX and XRD measurements, we confirmed HA formation on the honeycomb film. The peak intensities increased with an increase in the length of time for which hydrolysis and soaking in SBF were carried out, indicating that HA with higher crystallinity can be obtained by increasing the length of time for both hydrolysis and soaking. The process and kinetics of HA formation

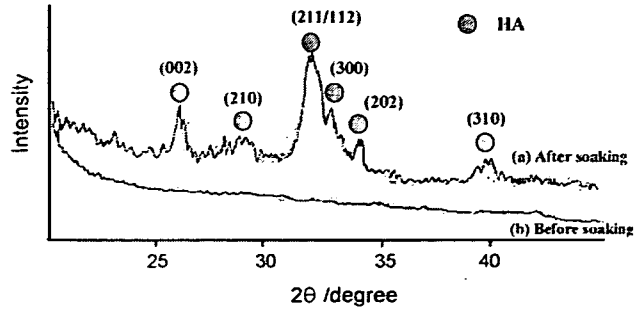

Fig. 5. XRD patterns of the honeycomb films that were first hydrolyzed for 360 min and then soaked in SBF. (a) Before soaking in SBF. (b) After soaking in SBF for 21 days.

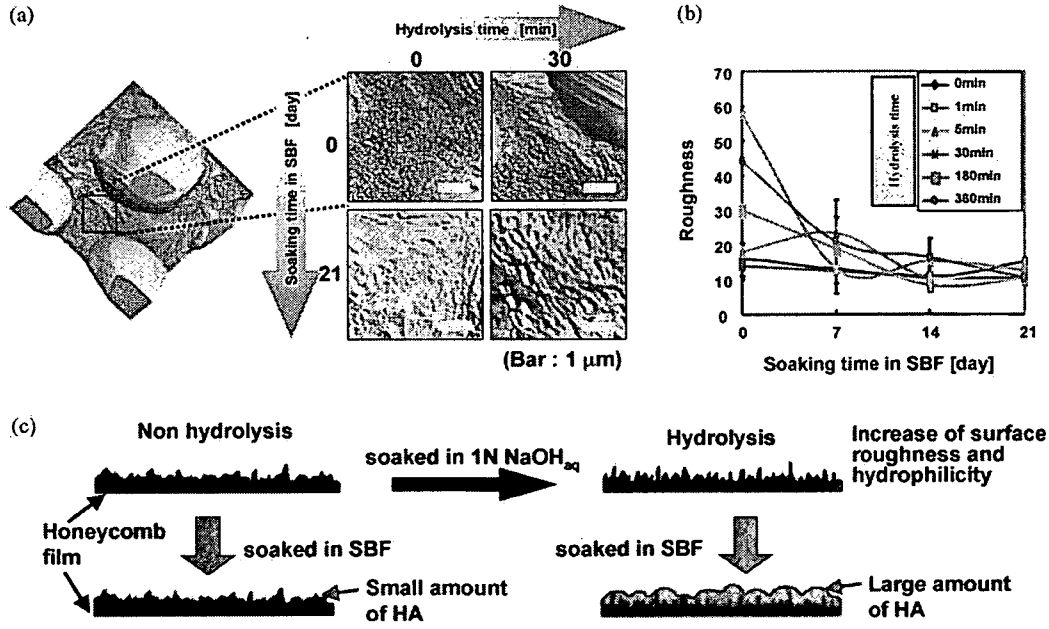

Fig. 6. (a) AFM images of the honeycomb films. (b) The relationship between surface roughness and soaking time. (c) Schematic representation of the cross-section of the honeycomb film covered with HA.

on honeycomb film could be affected by surface factors such as the density, surface area, composition, and structure (nano- and microstructure). In this study, the observed variations with time were in agreement with the nucleation and growth mechanism of an HA layer on substrates, as first reported by Kokubo and co-workers [23–28]. The AFM images (Fig. 6a) showed that the roughness of deposited HA on the honeycomb film was reduced as the soaking time in SBF was increased (Fig. 6b). This implies that the uniformity of HA that deposited on the honeycomb film depends on the length of time for which the films are soaked in SBF, as shown in Fig. 6c. The honeycomb film that was covered with HA was not swollen and retained a stable form in SBF. As mentioned above, bone tissue engineering is a promising approach for the treatment of defective and lost bone. Fabrication of biodegradable and biocompatible scaffolds with a 3D interconnected porous network has been a formidable challenge. This study shows the feasibility of fabricating cost-effective organic–inorganic scaffolds for tissue engineering to mimic bone by soaking films in SBF. The 3D porous honeycomb structure of a biodegradable scaffold was homogeneously mineralized using this HA formation technique at 37 °C. The polymer-HA composites thus obtained are expected to be useful as flexible bioactive bone-repairing scaffolds that can be processed in various shapes and be combined with various materials [33]. A biodegradable scaffold with sufficient bone cell compatibility (adhesion, proliferation, differentiation, and extracellular matrix secretion) and a suitable degradation rate, which could finally replace newly formed bone, is most desirable.

4. Conclusion

Formation of bone-like HA on a biodegradable honeycomb film was achieved under a biomimetic condition in which the PCL honeycomb film was modified with functional groups. The 3D porous structure of the PCL scaffold was homogeneously mineralized using this technique of HA formation. The HA crystal grew on the surface of the honeycomb films when the film was soaked in SBF. We clarified that the amount, uniformity, and crystallinity of HA were controlled by the length of time for which hydrolysis and soaking in SBF were carried out. These HA-deposited honeycomb films, which have the HA microstructure, could be useful as a flexible bioactive bone-repairing material.

Acknowledgements

This work is supported by Grants-in-Aid and CREST from Japan Science and Technology Corporation (JST), and Special Coordination Funds for Promoting Science and Technology of Ministry of Education, Culture, Sports, Science and Technology, Japan.

References

[1] S.J. Hollister, Nat. Mater. 4 (2005) 518.
[2] H.S. Nalwa (Ed.), Handbook of Nanostructured Biomaterials and Their Applications in Nanobiotechnology, vols. 1–2, American Scientific Pub., 2005.
[3] G.M. Whitesides, Small 1 (2005) 172.
[4] X. Jiang, D.A. Bruzewicz, A.P. Wong, M. Piel, G.M. Whitesides, Proc. Natl. Acad. Sci. 102 (2005) 975.
[5] A.G. Mikos, Y. Bao, L.G. Cima, J. Biomed. Mater. Res. 27 (1993) 183.
[6] M.J. Dalby, M.O. Riehle, D.S. Sutherland, H. Agheli, A.S.G. Curtis, Eur. Cell Mater. 9 (2005) 1.
[7] K. Whang, D.C. Tsai, E.K. Nam, M. Aitken, S.M. Sprague, P.K. Patal, K.E. Healy, J. Biomed. Mater. Res. 42 (1998) 491.
[8] C. Schugens, V. Maquet, C. Grandfils, R. Jerome, P. Teyssie, J. Biomed. Mater. Res. 30 (1996) 449.
[9] N. Maruyama, T. Koito, J. Nishida, T. Sawadaishi, X. Cieren, K. Ijiro, O. Karthaus, M. Shimomura, Thin Solid films 327/329 (1998) 854.
[10] O. Karthaus, N. Maruyama, X. Cieren, M. Shimomura, H. Hasegawa, T. Hashimoto, Langmuir 16 (2000) 6071.
[11] K. Sato, M. Tanaka, K. Hasebe, M. Takebayashi, K. Nishikawa, T. Kawai, M. Matsushita, S. Todo, M. Shimomura, Int. J. Nanosci. 1 (2002) 689.
[12] T. Nishikawa, R. Ookura, J. Nishida, K. Arai, J. Hayashi, N. Kurono, T. Sawadaishi, M. Hara, M. Shimomura, Langmuir 18 (2002) 5734.
[13] H. Yabu, M. Tanaka, K. Ijiro, M. Shimomura, Langmuir 19 (2003) 6297.
[14] M. Tanaka, M. Takebayashi, M. Miyama, J. Nishida, M. Shimomura, Bio-Med. Mater. Eng. 14 (2004) 439.
[15] A. Tsuruma, M. Tanaka, N. Fukushima, M. Shimomura, e.-J. Surf. Sci. Nanotechnol. 3 (2005) 159.
[16] H. Yabu, M. Takebayashi, M. Tanaka, M. Shimomura, Langmuir 21 (2005) 3235.
[17] J. Nemoto, Y. Uraki, T. Kishimoto, Y. Sano, R. Funada, N. Obata, H. Yabu, M. Tanaka, M. Shimomura, Bioresour. Technol. 96 (2005) 1955.
[18] Y. Fukuhira, E. Kitazono, T. Hayashi, H. Kaneko, M. Tanaka, M. Shimomura, Y. Sumi, Biomaterials 27 (2006) 1797.
[19] M. Tanaka, K. Nishikawa, H. Okubo, H. Kamachi, T. Kawai, M. Matsushita, S. Todo, M. Shimomura, Colloids Surf. A 284/285 (2006) 464.
[20] M. Tanaka, A. Takayama, E. Ito, H. Sunami, S. Yamamoto, M. Shimomura, J. Nanosci. Nanotechnol. 7 (2007) 763.
[21] L.L. Hench, R.J. Splinter, W.C. Allen, T.K. Greenlee, J. Biomed. Mater. Res. Symp. 2 (1972) 117.
[22] M. Jarco, J.F. Kay, K.I. Gumaer, R.H. Doremus, H.P. Drobeck, J. Bioeng. 1 (1977) 79.
[23] T. Kokubo, H. Kushitani, S. Sakka, T. Kitsugi, T. Yamamuro, J. Biomed. Mater. Res. 24 (1990) 721.
[24] H.M. Kim, F. Miyaji, T. Kokubo, T. Nakamura, J. Biomed. Mater. Res. 32 (1996) 409.
[25] T. Miyazaki, H.M. Kim, F. Miyaji, T. Kokubo, H. Kato, T. Nakamura, J. Biomed. Mater. Res. 50 (2000) 35.
[26] M. Tanahashi, T. Yao, T. Kokubo, M. Minoda, T. Miyamoto, T. Nakamura, T. Yamamuro, J. Am. Ceram. Soc. 77 (1994) 2805.
[27] M. Kawashita, M. Nakao, M. Minoda, H.M. Kim, T. Beppu, T. Miyamoto, T. Kokubo, T. Nakamura, Biomaterials 24 (2003) 2477.
[28] H.M. Kim, T. Himeno, T. Kokubo, T. Nakamura, Biomaterials 26 (2006) 4366.
[29] L.C. Bell, A.M. Posner, J.P. Quirk, Nature 239 (1972) 515.
[30] L.L. Hench, Bioceramics from concept to clinic, J. Am. Ceram. Soc. 74 (1991) 1487.
[31] L.L. Hench, J. Biomed. Mater. Res. 15 (1998) 511.
[32] T. Kokubo, H.M. Kim, M. Kawashita, Biomaterials 24 (2003) 2161.
[33] M. Tanaka, K. Yoshizawa, A. Tsuruma, S.Yamamoto, M. Shimomura, Japan Patent No. 2006-18260.

Available online at www.sciencedirect.com
ScienceDirect
Colloids and Surfaces A: Physicochem. Eng. Aspects 313–314 (2008) 530–535
COLLOIDS AND SURFACES A
www.elsevier.com/locate/colsurfa

Effect of pore size of honeycomb films on the morphology, adhesion and cytoskeletal organization of cardiac myocytes

Keiko Arai [a,*], Masaru Tanaka [b], Sadaaki Yamamoto [c], Masatsugu Shimomura [a,b]

[a] *Frontier Research System, RIKEN, Hirosawa 2-1 Wako, Saitama 351-0198, Japan*
[b] *Nanotechnology Research Center, Research Institute for Electronic Science, Hokkaido University, N21W10 Kita-ku, Sapporo 001-0021, Japan*
[c] *Creative Research Initiative "Sousei", Hokkaido University, N21W10 Kita-ku, Sapporo 001-0021, Japan*

Received 17 November 2006; accepted 30 April 2007
Available online 2 June 2007

Abstract

Cells respond to the circumstances such as structures and chemical composition of scaffolds and cytokine. In this report, the responses of cytoskeleton and spreading of cardiac myocytes to the self-organized honeycomb-patterned films (honeycomb films) of biodegradable poly(ε-caprolactone) (PCL) with several pore sizes were investigated. The expression of actin filament of cardiac myocytes was strongly dependent on the pore size ranging from 4 to 13 μm. Immunofluorescent labeling of vinculin in cardiac myocytes showed localization of focal contact along the edge of the honeycomb pores. The results indicated that the honeycomb structures and the pore sizes influence the morphology, cytoskeletal organization and focal adhesion of the cardiac myocytes.

Keywords: Cardiac tissue engineering; Cell morphology; Cell adhesion; Micropatterning; Scaffold; Honeycomb film; Cardiac myocytes

1. Introduction

The influence of micropatterned substrates on cellular morphology is of an ongoing interest in the fields of tissue engineering and biosensing [1–3]. Micropatterned substrates are potential scaffolds for regeneration of cardiac and fibrous tissues, which have an ordered structure. Micro-contact printing and photolithography have been applied to the fabrication of micropatterned surfaces for ordered tissue regeneration [4–8].

We reported that honeycomb-patterned polymer films (honeycomb films) can be prepared by casting functionally selected polymer, dissolved in a water-immiscible solvent under high humidity [9–16]. Moreover, the pore size of the films can be controlled from hundreds of nanometers to hundreds of microns. These films has been fabricated from various polymers and be self-supported. This technology was adopted for biological applications. Specifically, the morphology and, in turn, the function of hepatocytes, endothelial and neural projenitor cells were all controlled by manipulating the size of the micropores on the honeycomb films [9,14,16–22].

The alignment and function of myocytes have been controlled in vivo. Understandably, these achievements are vital in the field of cardiac regeneration [15]. In this study, we investigated the possibility to control the morphology and cytoskeletal function of cardiac myocytes by manipulating of pore size of honeycomb films. In doing so, cardiac myocytes were cultured on the honeycomb films with three different pore size (subcellular, cellular and overcellular size). We examined the influence of the pore size on the morphology, cytoskeleton and focal adhesion of cardiac myocytes using a confocal laser scanning microscope and a scanning electron microscope.

2. Experiment

2.1. Preparation of self-supported honeycomb films

Polymers used for the preparation of self-supported honeycomb films were poly(ε-caprolactone) (PCL, Wako, Mw: 70,000–100,000, Fig. 1(1)), and an amphiphilic copolymer (M_w: 19,700, Fig. 1(2)) synthesized according to the procedure previously reported [23]. Honeycomb films were fabricated according to the method reported previously [16]. Briefly, polymer solution containing PCL (1 mg/ml) and the copolymer (0.1 mg/ml) was

* Corresponding author. Tel.: +81 48 462 1111; fax: +81 48 462 4695.
E-mail address: akeiko@riken.jp (K. Arai).

0927-7757/$ – see front matter © 2007 Elsevier B.V. All rights reserved.
doi:10.1016/j.colsurfa.2007.04.128

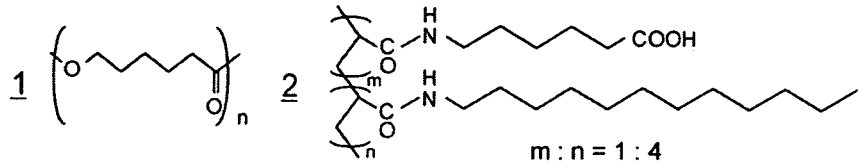

Fig. 1. Chemical structures of biodegradable poly(ε-caprolacton) (1) and amphiphilic copolymer (2), both of which were used to manufacture the honeybomb films.

prepared by dissolving each polymer in chloroform. In order to prepare honeycomb films with a variety of pore size, 3–15 ml of the mixed solution was cast onto 9 cm diameter glass petri dish under high humidity (80% r.h.) at 20 °C. These films were peeled off from a glass substrate and supported by two Teflon sheets with a 6 mm diameter hole (hereafter called self-supported honeycomb film) (Fig. 2). Flat films consisting of same polymers that have no microporous structure were prepared on a glass substrate by casting under dry conditions (20% r.h.) at 20 °C. Then the polymer films were peeled off from a glass substrate and put on a polystyrene Petri dish. The surface morphology of the films was observed by optical microscopy (BX60, Olympus) and scanning electron microscopy (SEM; S-3000N, Hitachi). Before cell culture, these films were sterilized by ethylene oxide gas at 40 °C for 2 h, followed by the evacuation for 20 h. The sterilized films were pre-incubated in culture medium overnight.

2.2. Cell culture

Cardiac myocytes were isolated from hearts of 19-day embryos rat [24]. The hearts of embryonic Sprague Dawley rats (Japan SLC Inc.) were removed under sterile conditions. Each heart was washed in a Petri dish containing Ca/Mg-free Hanks balanced salt solution (HBSS; GIBCO BRL). Then the hearts were massaged to remove blood and minced with a scalpel blade. The minced hearts were washed three times in ice-cold HBSS. The HBSS was replaced with 0.05% crude trypsin (Sigma–Aldrich) in versene buffer (GIBCO). After 20 min of incubation at 37 °C, the supernatant was discarded. The minced hearts were enzymatically treated by DNase TypeII solution (10,000 unit/ml, Sigma) for 1–2 min, then by addition of 0.05% trypsin/versene for 20 min at 37 °C. The supernatant of the cell suspension was added to Hepes-buffered Hams F10 medium containing 0.5% insulin-transferrin-selenium-X solution (ITS-X; GIBGO) and 10% fetal calf serum (FCS; GIBCO) to block trypsinization. The supernatant was centrifuged for 5 min at 100 × *g* control, resuspended in ice-cold Hepes-buffered Hams F10 containing 0.5% ITS-X and 10% FCS. The cell suspension was stored at 0–4 °C until the next process. The collected cell suspensions were pooled in a 25 cm^2 tissue culture flask and incubated for 30 min at 37 °C. This incubation allowed the majority of cell debris and fibroblasts to adhere to the flask, and resulted in the concentration of myocytes in the cell suspension. Finally the cardiac myocytes were seeded onto the pre-fabricated matrices at the density of 3.0×10^4 cells/cm^2. The cell morphology was observed by optical microscopy (IX70, Olympus) and SEM.

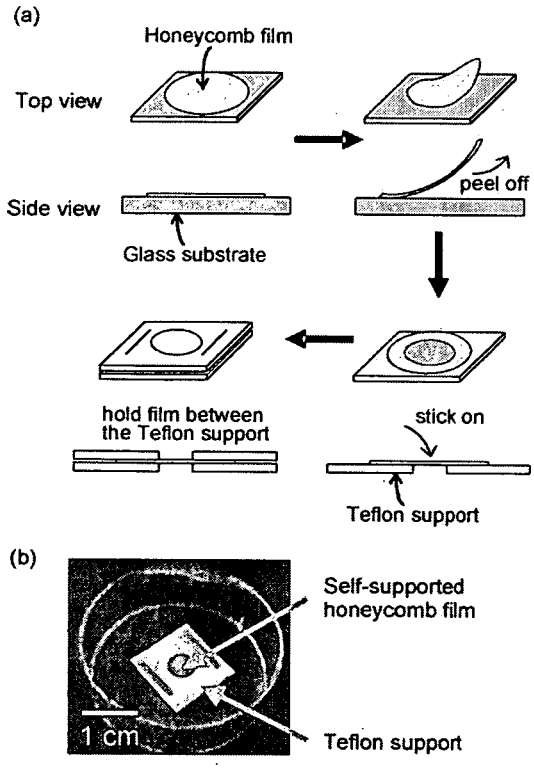

Fig. 2. Schematic illustration of scaffold preparation (a) and whole view of self-supported honeycomb film (b).

2.3. SEM measurement

Cultured cardiac myocytes were washed with PBS and fixed with 1.25% glutal aldehyde in PBS. After washing with PBS, the samples were dehydrated by immersing in increasing ethanol concentration solution gradually and *t*-butylalchol, and were then freeze dried For SEM imaging, the samples were sputter-coated with platinum-palladium using a commercially available unit (Hitachi E1030, Hitach, Japan). SEM images were obtained using a Hitachi S-3000N SEM (Hitachi, Japan) at an acceleration voltage of 15 kV.

2.4. Immunofluorescence analysis

Cardiac myocytes were cultured on the flat and honeycomb films. The cells were fixed with 4% paraformaldehyde (SIGMA) for 10 min and permeated with 1% tritonX-100 (SIGMA) for 10 min. After blocking with 5% bovine serum albumin in phosphate-buffered saline (PBS) for 30 min, cells were incubated for 1.5 h with mouse monoclonal anti vinculin IgG1 antibodies (CHEMICON International Inc.) at 37 °C. After washing with PBS, the vinculin complexes were visualized by

incubation with Alexa Fluor 488 anti-mouse IgG antibodies (Molecular Probes) for 1 h at 37 °C. The cells were treated with 1 μg/ml rhodamine-conjugated phalloidine (Molecular Probes) solution, incubated at 37 °C for 45 min and washed with PBS three times. The samples were observed with confocal laser scanning microscope (CLSM) (FV300, Olympus).

3. Results and discussion

3.1. Surface morphology of honeycomb films

The formation process of the honeycomb films has been reported previously [15]. We determined the diameter of honeycomb pores and width of honeycomb film by the average of 5-point measurement from SEM image. The honeycomb films had pore sizes in the range of 4–13 μm. The widths of the rim (Fig. 3) were 1.50 ± 0.5, 3.00 ± 0.50 and 8.00 ± 0.50 μm, respectively. The size of cardiac myocytes was the range of 7–10 μm in diameter. Here, we classified the films as subcellular (4.00 ± 0.50 μm), cellular (8.00 ± 0.50 μm) and overcellular (12.5 ± 0.50 μm) size in comparison to the size of the cell, respectively (Fig. 3). The porosity of the honeycomb films was approximately 50% irrespective of the pore size. The porosity implies that the area of honeycomb films on which cells adhere was half of the flat film.

3.2. Morphology, cytoskeleton and focal contact of cardiac myocytes on honeycomb films

It is known that a morphology of cells changes depending on the adhesion area [1–6]. The morphology, cytoskeleton and adhesion of the cardiac myocytes on the self-supported honeycomb films and the flat film were compared. As there were no significant differences in cell morphology at days 1, 3, and 5, we showed their morphology at day 5 as a representative image of this culture period (Fig. 4). SEM observation revealed that the cell morphologies were dependent on the pore size (Fig. 4). On the flat, subcellular and cellular pore size honeycomb films, the uniaxially elongating (U) and multi directionally spreading (M) cells were observed (Fig. 4(a)–(c)). Many cells spread across several pores on subcellular pore size honeycomb films. On the overcellular pore size films, the cells extended their body along the micropores and showed uniaxially elongating shape (Fig. 4(d)).Although the cell morphology was independent on culture time, the development of cytoskeleton and focal adhesion point were strongly dependent on culture time. Fig. 5 is the CLSM images showing vinculin and cytoskeleton of the cells at 1 day and 3 days culture after seeding. Vinculin is a protein in focal adhesion complexes. The vinculin expression shows the adhesion area of cells to extracellular matrix. On the flat film, vinculin was located randomly over entire

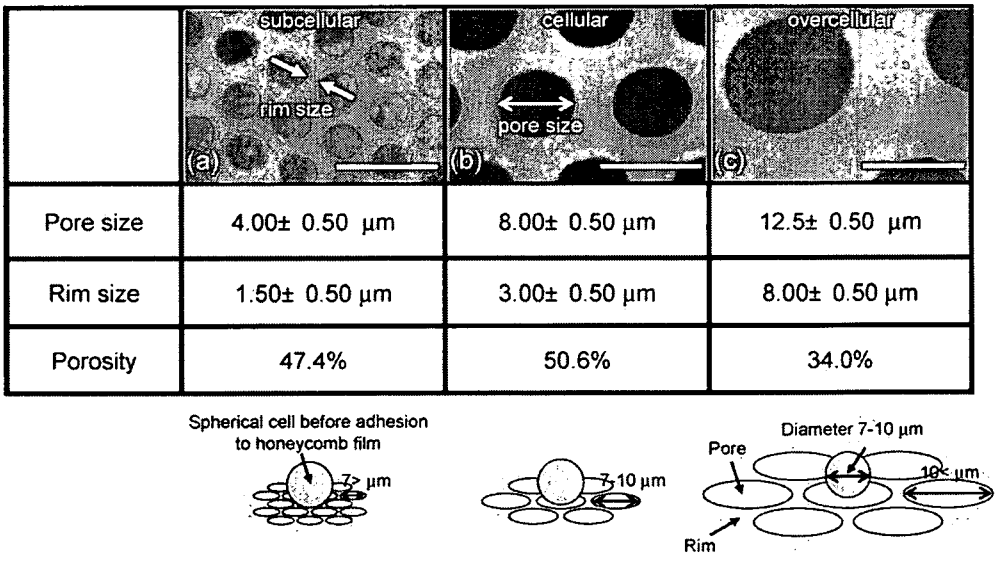

	subcellular	cellular	overcellular
Pore size	4.00± 0.50 μm	8.00± 0.50 μm	12.5± 0.50 μm
Rim size	1.50± 0.50 μm	3.00± 0.50 μm	8.00± 0.50 μm
Porosity	47.4%	50.6%	34.0%

Fig. 3. SEM images of the self-supported honeycomb films with (a) subcellular size, (b) cellular size and (c) overcellular size pores. Bar: 10 μm.

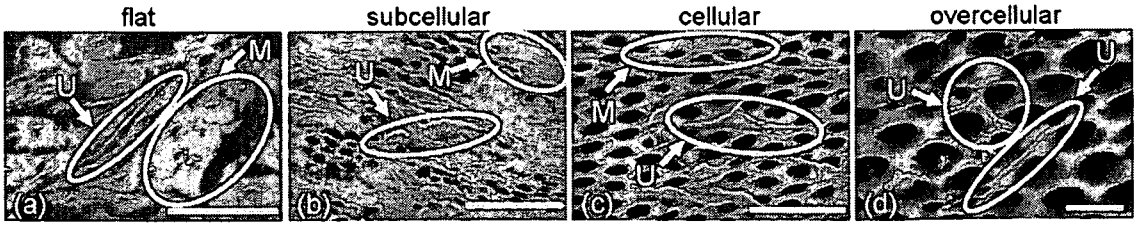

Fig. 4. SEM images of cells on the flat film and the honeycomb films with each pore sizes (a)–(d) in 5 days culture. M, Multi-directionally spreading; U, uniaxially spreading. Bar: 30 μm.

cell bodies along the actin filaments, irrespective of culture time (Fig. 5(a)). On the honeycomb films, vinculin was localized at the edge of the honeycomb pores irrespective of pore size (Fig. 5(b)–(d)). U-3 in Fig. 5(d) shows localization of the vinculin cluster along the edge of the honeycomb pores. The development of vinculin on the subcellular and cellular pore size honeycomb films was dependent on culture time. Vinculin was faint and did not organize clearly after 1-day culture (M-1, U-1 in Fig. 5(b) and (c)). The size and the number of vinculin cluster were restricted. However after 3 days culture, vinculin cluster became clear and grew (M-3, U-3 in Fig. 5(b) and (c)). On the overcellular pore size films, vinculin clusters were clearly and well organized (U-1, U-3 in Fig. 5(d)), irrespective of culture time. Our recent investigation revealed that cell adhesion protein, fibronectin molecule adsorb around the pore periphery of a honeycomb film [16,17]. Thus, the location of focal contact at the periphery of the pore can be ascribed to the binding between cell surface protein, integrin and fibronectin at the periphery of the pore. This suggests that the spreading direction of the cardiac myocytes can be controlled by the alignment of the pore.

On the flat film, actin filaments were clear and well organized along elongated direction of a cell (Fig. 5(e)), irrespective of culture time. Actin fibers were thick and anisotropic and were

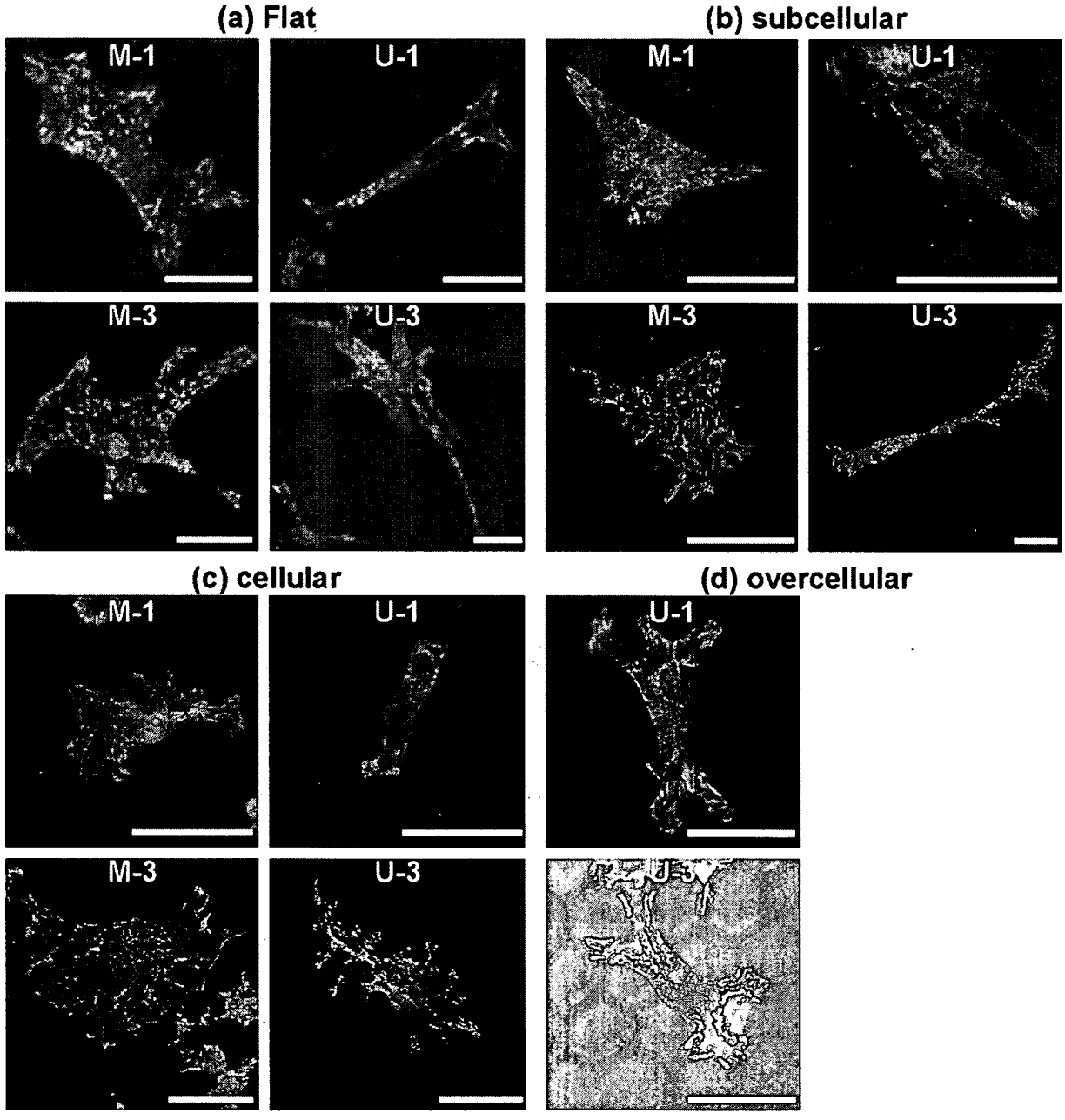

Fig. 5. Immunofluorescence images of cardiac myocytes on the flat film (a and e) and the self-supported honeycomb films with subcellular (b and f), cellular (c and g) and overcellular (d and h) pore sizes in 1-day culture (M-1, U-1) and 3 days culture (M-3, U-3). M, Multi-directionally spreading; U, uniaxially spreading; green, vinculin; red: actin. Immunofluorescence image in (d) U-3 is superimposed on a differential interference microscope image of a honeycomb film showing that vinculin was localized along the edge of the honeycomb pores.

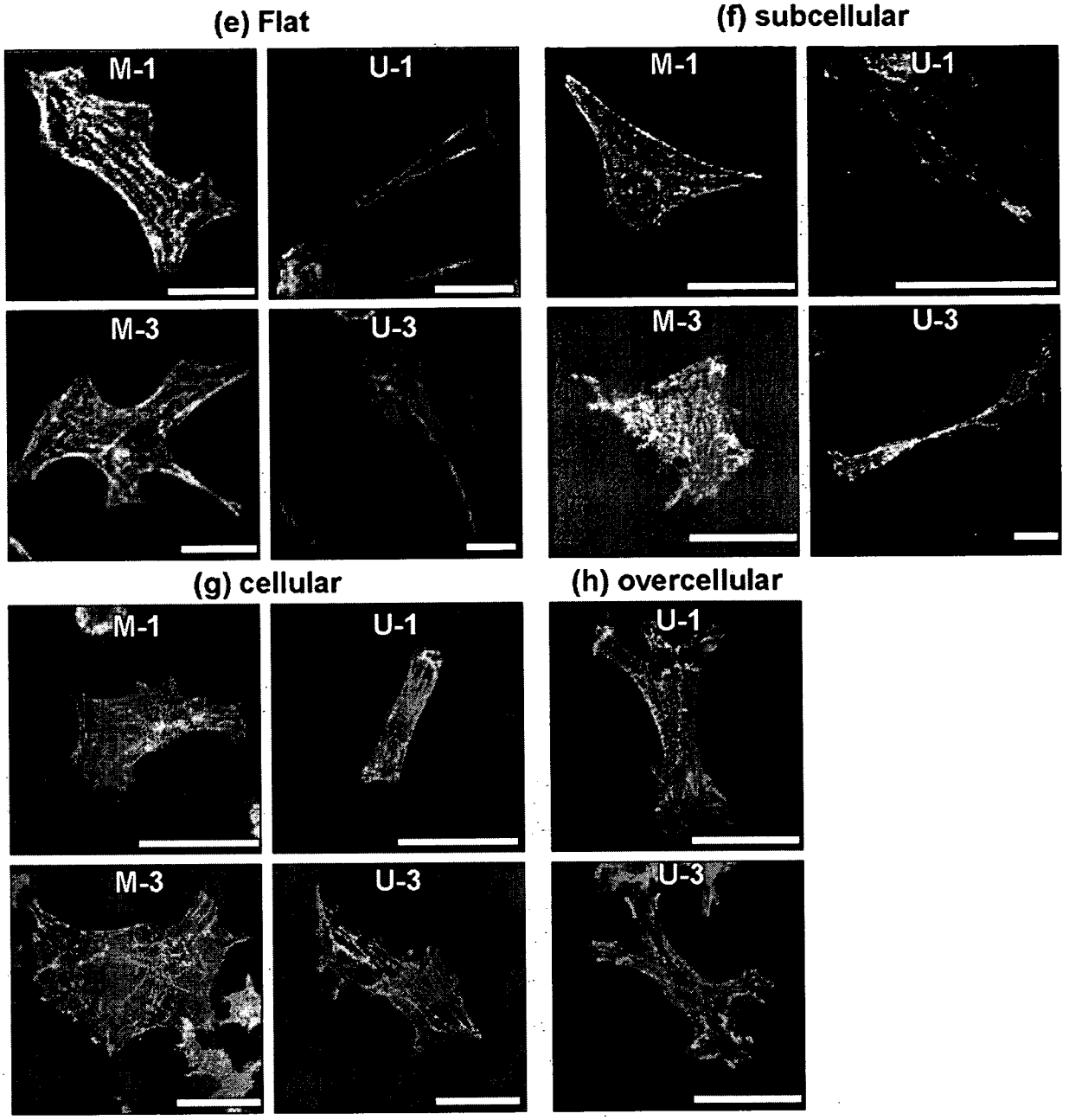

Fig. 5. (*Continued*).

observed cross striation. The morphology and adhesion behavior per cell of 1 day and 3 days culture were almost the same when compared M-1, U-1 with M-3, U-3 in Fig. 5(f) and (g) on the subcellular and cellular pore size films. Actin fibers were faint and did not organize clearly after 1-day culture and their direction was random (M-1, U-1 in Fig. 5(f) and (g)). However, after 3 days culture, the cells with clear and random actin fibers were coexisted (M-3, U-3 in Fig. 5(f) and (g)). The development and alignment of actin fiver were also dependent on culture time. On the overcellular pore size films, actin filaments were clear and well organized along elongated direction of a cell (Fig. 5(h)), irrespective of culture time.

The morphology of cardiac cells was controlled by the large pore of honeycomb structures. On the film with overcellular pore size, the morphology was only U type, whereas on the other films, the morphology had both M and U types (see Figs. 4 and 5). The honeycomb films have approximately half adhesion area compared with the flat film and provide the restricted adhesion site that is located at the periphery of the pore. In addition, it is probably difficult for the cells to cross the large pores. It may follow from these adhesion condition characteristic to the honeycomb films that the cells were forced to elongate along the rims of honeycomb structures. The cardiac cells construct fibrous texture in the living body [25]. The cardiac cells showed well-organized actin filaments and preferentially uniaxially elongated morphology on the honeycomb films with the pores of overcellular size, suggesting that the honeycomb films can control the spreading of the cardiac myocytes and organization of actin fil-

aments by controlling the pore size, giving fibrous texture like in the living body.

4. Conclusion

In the present study, the effect of pore sizes of the honeycomb films on the morphology of cardiac myocytes was demonstrated. The dependence of the morphology on the pore size may be associated with the adhesion condition characteristic to the honeycomb films, namely, limited adhesion site along the periphery of the pore, small adhesion area and difficulty of cellular migration on the porous surface. In addition to the previous study, based on pore morphology, we found that honeycomb film demonstrates potentials good for regenerating cardiac tissue, the efficiency of which may be controlled by manipulating the size and shape of the pores on the films.

Acknowledgements

This work is supported by Grants-in-Aid from Japan Science and Technology Corporation (JST) and Special Coordination Funds for Promoting Science and Technology of Ministry of Education, Culture, Sports, Science and Technology.

References

[1] R. Singhvi, A. Kumar, G.P. Lopez, G.N. Stephanopoulos, D.I. Wang, G.M. Whitesides, D.E. Ingber, Science 264 (1994) 696.
[2] C.A. Thomas Jr., P.A. Springer, G.E. Loeb, Y. Berwald-Netter, L.M. Okun, Exp. Cell Res. 74 (1972) 61.
[3] S. Britland, E. Perez-Arnaud, P. Clark, B. McGinn, P. Connolly, G. Moores, Biotechnol. Prog. 8 (1992) 155.
[4] D.E. Ingber, Proc. Natl. Acad. Sci. USA 87 (1990) 3579.
[5] K.L. Prime, G.M. Whitesides, Science 252 (1991) 1164.
[6] R. Vaidya, L.M. Tender, G. Bradley, M.J. O'Brien II., M. Cone, G.P. Lopez, Biotechnol. Prog. 14 (1998) 371.
[7] D. Motlagh, T.J. Hartman, T.A. Desai, B. Russell, J. Biomed. Mater. Res. Part A 67 (2003) 148.
[8] D. Motlagh, S.E. Senyo, T.A. Desai, B. Russell, Biomaterials 24 (2003) 2463.
[9] T. Nishikawa, J. Nishida, R. Ookura, S. Nishimura, S. Wada, T. Karino, M. Shimomura, Mater. Sci. Eng. C8–9 (1999) 495.
[10] T. Nishikawa, J. Nishida, R. Ookura, S. Nishimura, S. Wada, T. Karino, M. Shimomura, Mater. Sci. Eng. C10 (1999) 141.
[11] K. Sato, K. Hasebe, M. Tanaka, M. Takebayashi, K. Nishikawa, M. Shimomura, T. Kawai, M. Matsushita, S. Todo, Int. J. Nanosci. 1 (2002) 689.
[12] F.A. Denis, P. Hanarp, D.S. Sutherland, J. Gold, C. Mustin, P.G. Rouxhet, Y.F. Dufrêne, Langmuir 18 (2002) 819.
[13] N. Maruyama, T. Koito, J. Nishida, T. Sawadaishi, X. Cieren, K. Ijiro, O. Karthaus, M. Shimomura, Thin Solid Films 327–329 (1998) 854.
[14] T. Nishikawa, R. Ookura, J. Nishida, K. Arai, J. Hayashi, N. Kurono, T. Sawadaishi, M. Hara, M. Shimomura, Langmuir 18 (2002) 5734.
[15] T. Nishikawa, M. Nonomura, K. Arai, K. Hayashi, T. Sawadaishi, Y. Nishiura, M. Hara, M. Shimomura, Langmuir 19 (2003) 6193.
[16] M. Tanaka, M. Takebayashi, M. Miyama, J. Nishida, M. Shimomura, Bio-Med. Mater. Eng. 14 (2004) 439.
[17] A. Tsuruma, M. Tanaka, N. Fukushima, M. Shimomura, e-J. Surf. Sci. Nanotechnol. 3 (2005) 159.
[18] T. Nishikawa, J. Nishida, R. Ookura, H. Ookubo, H. Kamachi, M. Matsushita, S. Todo, M. Shimomura, Stud. Surf. Sci. Catal. 132 (2001) 509.
[19] M. Tanaka, K. Nishikawa, H. Okubo, H. Kamachi, T. Kawai, M. Matsushita, S. Todo, M. Shimomura, Coll. Surf. A 284–285 (2006) 464.
[20] H. Sunami, E. Ito, M. Tanaka, S. Yamamoto, M. Shimomura, Coll. Surf. A 284–285 (2006) 548.
[21] S. Yamamoto, M. Tanaka, H. Sunami, K. Arai, A. Takayama, S. Yamashita, Y. Morita, M. Shimomura, Surf. Sci. 600 (2006) 3785.
[22] M. Tanaka, A. Takayama, E. Ito, H. Sunami, S. Yamamoto, M. Shimomura, J. Nanosci. Nanotechnol. 7 (2007) 763.
[23] S. Nishimura, K. Yamada, J. Am. Chem. Soc. 119 (1997) 10555.
[24] M.C.T. Denyer, M. Riehle, J. Hayashi, M. Scholl, C. Sproessler, S.T. Britland, A. Offenhaeusser, W. Knoll, In Vitro Cell, Dev. Biol.-Anim. 35 (1999) 352.
[25] N.J. Severs, Bio Essays 22 (2000) 188.

Available online at www.sciencedirect.com
ScienceDirect
Colloids and Surfaces A: Physicochem. Eng. Aspects 313–314 (2008) 520–525
COLLOIDS AND SURFACES A
www.elsevier.com/locate/colsurfa

Effect of honeycomb-patterned structure on chondrocyte behavior in vitro

Yukako Fukuhira[a,b,*], Hiroaki Kaneko[a], Mika Yamaga[a], Masaru Tanaka[b], Sadaaki Yamamoto[c], Masatsugu Shimomura[b]

[a] *Department of Tissue Engineering Development, Innovation Research Institute, Teijin Ltd., Tokyo 191-8125, Japan*
[b] *Nanotechnology Research Center, Research Institute for Electronic Science, Hokkaido University, Sapporo 060-0812, Japan*
[c] *Creative Research Initiative "Sousei", Hokkaido University, Sapporo 060-0812, Japan*

Received 19 November 2006; accepted 23 April 2007
Available online 2 June 2007

Abstract

Chondrocytes were cultured on a honeycomb-patterned poly(lactic acid) (PLA) film in order to evaluate the effects of the honeycomb structure on chondrocytes with regard to cell proliferation, the production of sulphated glycosaminoglycans (sGAG), and morphological behavior. Cell proliferation was evaluated using the alamar blue assay, and sGAG production was spectrophotometrically quantified. Cell morphology was observed by means of optical microscopy (OM) and transmission electron microscopy (TEM). In comparison to the honeycomb-patterned film, the flat film showed significantly higher levels of chondrocyte growth; however, chondrocytes were flattened in a manner similar to that of fibroblasts and produced small amounts of extracellular matrix (ECM). On the contrary, chondrocytes cultured on the honeycomb-patterned film were observed to remain spherical shaped and produce ECM abundantly. The results indicate that the honeycomb-patterned structure reduced the points of attachment for the chondrocytes and that they have the potential to provide chondrocytes with a suitable environment for developing a spherical shape. The honeycomb-patterned structure of the PLA film may play an important role in determining chondrocyte behavior and as a scaffold that can be used in tissue engineering.

Keywords: Chondrocyte; Self-organization; Cell morphology; Honeycomb-patterned film

1. Introduction

Surface chemistry and topology are important factors with regard to the biocompatibility and performance of tissue engineering scaffolds. Surface modification methods are thus required to suppress adverse effects and trigger a specific biological response such as the promotion of cell growth, cell migration, cell differentiation, and ECM production. Various types of methods to modify the surface properties of the scaffolds such as lithography, micro-contact printing, phase separation, and salt leaching [1–5]. We have already reported that honeycomb-patterned structures on polymer films are fabricated by using a simple casting method [6,7]. The honeycomb-patterned film affects cell morphology, for example, hepatocytes form a spherical shape on the honeycomb-patterned film; moreover, hepatic function is enhanced [8]. To form the honeycomb pattern on a polymer film, a surfactant is essential for stabilizing the water droplets; further, it acts as a template for the honeycomb pattern on the surface of the polymer solution. The surfactant must possess amphiphilicity, because it contributes to the stability of the water droplet at the polymer solution–water interface. Thus far, the amphiphilic poly(acrylamide) copolymer (CAP), which is derived from dodecylacrylamide and ω-carboxyhexylacrylamide, has been reported as the only surfactant useful for creating the honeycomb pattern on a biodegradable polyester [9]. We discovered that dioleoylphosphatidylethanolamine (DOPE) is suitable as a novel surfactant for fabricating the honeycomb-patterned PLA film (HC-PE), which exhibited greater proliferation and adhesion of NIH3T3 cells than that on the honeycomb-patterned PLA film with CAP (HC-CAP) [7].

Articular cartilage contains a small number of chondrocytes in ECM that are mainly composed of water, collagen II, proteoglycans, and several other classes of molecules, including

* Corresponding author at: Department of Tissue Engineering Development, Innovation Research Institute, Teijin Ltd., 4-3-2, Asahigaoka, Hino, Tokyo 191-8125, Japan. Tel.: +81 42 586 8426; fax: +81 42 587 5511.
E-mail address: y.fukuhira@teijin.co.jp (Y. Fukuhira).

0927-7757/$ – see front matter © 2007 Elsevier B.V. All rights reserved.
doi:10.1016/j.colsurfa.2007.05.047

lipids, phospholipids, proteins, and glycoproteins. Chondrocytes are generally spherical shaped; however, their shapes become a more like fibroblasts when they are isolated and are cultured on a culture plate [10]. Therefore, maintaining the cell morphology and promoting the ECM production of the cultured cells are important factors for tissue engineering [11–15]. The scaffolds must be highly porous in order to maintain cell morphology and regenerate ECM [16].

In this study, we have investigated the effects of the honeycomb-patterned film on chondrocytes with regard to cell proliferation, sGAG production, and morphological behavior. In addition, the influence of the differing surfactant properties of HC-PE and HC-CAP on chondrocyte behavior was evaluated.

2. Experimental

2.1. Preparation of honeycomb-patterned and flat films

HC-PE was prepared as previously described [7]. The pattern of each film was observed using an optical microscope (OM) (BX51; Olympus, Tokyo, Japan). The honeycomb-patterned films were obtained as a highly regular hexagonal structure comprising pores with a diameter of 5 μm (Fig. 1). CAP, which was used as a surfactant in the fabrication of the honeycomb-patterned films, was synthesized according to a previously reported procedure [17]. The method for fabricating HC-CAP is identical to that used for HC-PE. The flat film was prepared from of PLA and PE by using a casting method without surface modifications.

2.2. Cell preparation

Chondrocytes were isolated from New Zealand white rabbit articular cartilage. Briefly, cartilage tissue obtained from the rabbit knee was cut into small pieces and then washed with 0.2% glucose in phosphate-buffered saline (PBS). The chondrocytes were isolated by incubating the cartilage pieces in PBS containing 0.25% trypsin-EDTA and 0.2% glucose at 37 °C for 1 h. Subsequently, the chondrocytes were incubated in α-MEM (Invitrogen) containing 0.15% collagenase type II at 37 °C for 2 h. The chondrocytes were grown in α-MEM supplemented with 10% heat inactivated fetal bovine serum (Hyclone, UT, USA), 1% penicillin-streptomycin, and 25 μg/mL L(+)-ascorbic acid. Each film coated on cover glasses (1.13 cm^2), which were fixed between 2 stainless rings in order to prevent them from floating in the culture medium. These films were sterilized in 70% ethanol, immersed in PBS and α-MEM and set in a 6-well culture plate. The chondrocytes were seeded on each film in the culture media to give a final density of 1.3×10^4 cells/cm^2 and incubated at 37 °C in an atmosphere of 5% CO_2 in air, and the media were changed every 2 days.

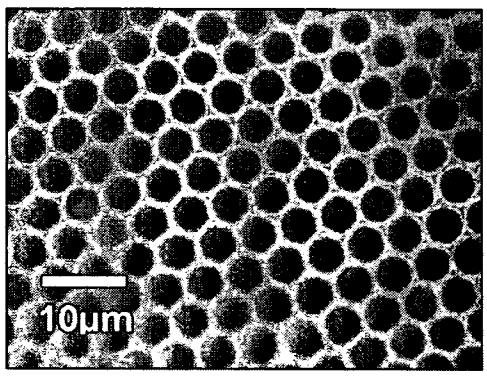

Fig. 1. OM image of the honeycomb-patterned film using DOPE as the surfactant.

2.3. Cell proliferation assay

Cell proliferation was quantitatively measured using the alamarBlue™ (Alamar Biosciences Inc., CA, USA) assay as described previously [7]. Briefly, after 3 and 10 days culture periods, alamarBlue™ was added to each well in an amount equal to 10% of the total culture medium volume, and the wells were then incubated for 2 h. Aliquots of 100 μL per sample were measured by using a fluorescence plate reader (Fusion™ αHT; Packard BioScience Company, CT, USA) set at excitation and emission wavelengths of 540 and 590 nm, respectively.

2.4. sGAG assay

An sGAG assay kit (Blyscan; Accurate Chemical & Scientific, Westbury, NY) was used for the quantitation of total sGAG in each culture. The sGAG produced by each culture were extracted by following a modified method described in a previous report [12]. Briefly, the chondrocytes were harvested on each film, washed with PBS, and digested with 500 μg/mL proteinase K in 100 mM sodium phosphate, pH 7.1, 5 mM EDTA4Na, and distilled water at 60 °C for 18 h. The extract was analyzed for the presence of sGAG and DNA. For the sGAG assay, the sample was reacted with the Blyscan dye reagent, composed of 1,9-dimethylmethylene blue, for 30 min, and the unbound dye solution was removed by centrifugation. Bound dye was released from the insoluble sGAG-dye complex and quantified spectrophotometrically based on A_{656} (Spectra® Max; Molecular Devices, CA, USA). The total amount of sGAG was calculated using a standard curve with chondroitin 4-sulfate as the standard.

2.5. DNA content

DNA analysis was performed using the PicoGreen® dsDNA quantitation reagent (Molecular Probes, Inc., OR, USA), and the results were used to normalize the amount of sGAG. For the measurement of the DNA amount, 50 μL extract was added to the assay plate together with the PicoGreen fluorescent dye solution. The PicoGreen–DNA complex was measured using a fluorescence plate reader set at excitation and emission wavelengths of 490 and 520 nm, respectively. The total amount of DNA in the sample was determined using the standard provided in the kit.

2.6. Cell morphology

The cells that were cultured 2 weeks after seeding were fixed in 2.5% glutaraldehyde in PBS. For observation under

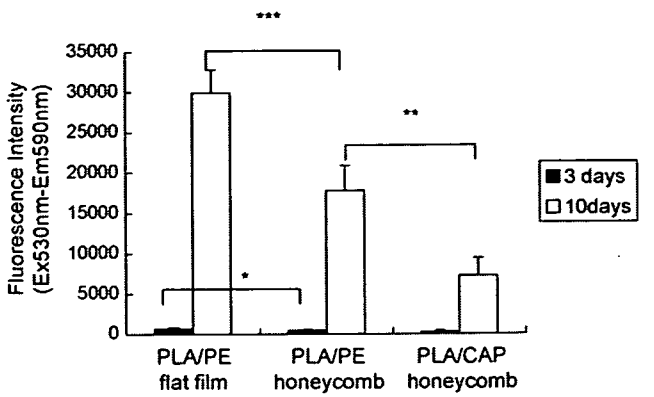

Fig. 2. Cell proliferation of the chodrocytes cultured on each film estimated by alamarBlue™ assay (*$p < 0.05$ (3 days) and ***$p < 0.001$ (10 days), the flat film is significantly different compared with HC-PE; **$p < 0.01$ (10 days), HC-PE is significantly different as compared with HC-CAP).

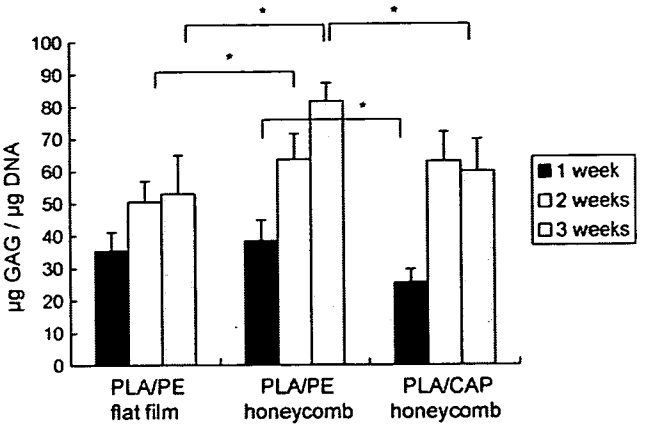

Fig. 3. sGAG content of the chondrocytes cultured on each film (*$p < 0.05$ (2 and 3 weeks), HC-PE is significantly different as compared with the flat film; *$p < 0.05$ (1 and 3 weeks), HC-PE is significantly different as compared with HC-CAP).

OM, the samples were stored overnight at 4 °C followed by refixation with 1% solution of osmium(VIII)oxide. Subsequently, the samples were dehydrated by a step-wise treatment with ethanol, embedded in mixed resin (QY-2 and Epon) (Nissin EM Corporation, Tokyo, Japan), and cut into 1-μm thick slices with a microtome. After staining with toluidine blue, the samples were analyzed by OM. For observation under TEM, after embedding, the above samples were also cut into 50-nm thick slices. After staining with 4% uranylacetate and 0.5% lead citrate, the samples were analyzed by TEM.

2.7. Statistical analysis

Numerical data were evaluated by using analysis of variance using a generally available commercial statistical software package. A p value of less than 0.05% was regarded as statistically significant.

3. Results and discussions

3.1. Cell proliferation

Chondrocyte proliferation was evaluated using the alamarBlue™ assay and is summarized in Fig. 2. After 3 days of cell culture, cell proliferation was significantly higher on the flat film than that on HC-PE ($p < 0.05$). Moreover, cell proliferation on HC-PE was slightly higher than that on HC-CAP. After 10 days of cell culture, cell proliferation on each film exhibited tendencies identical to those observed at 3 days

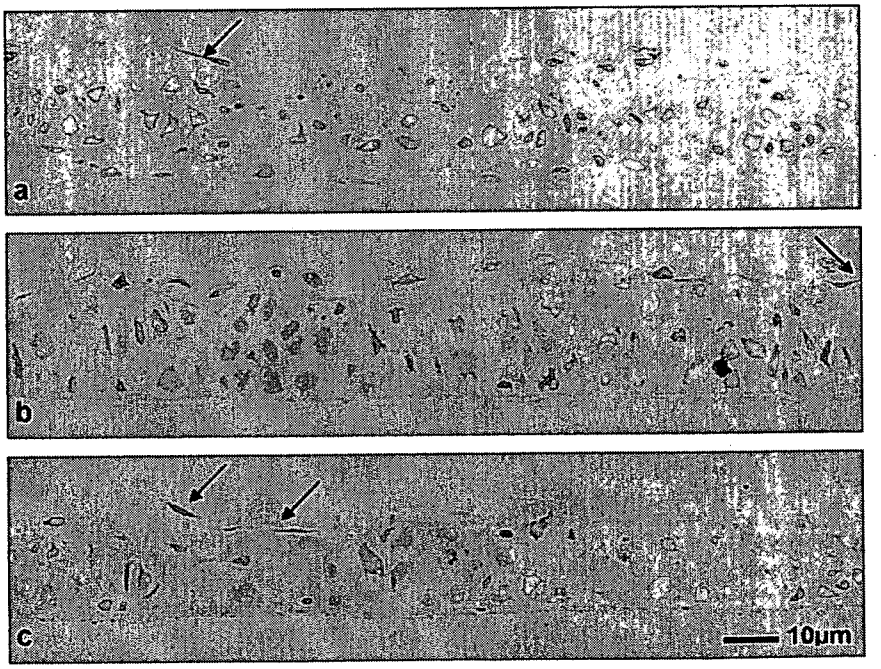

Fig. 4. Toluidine blue-stained section of the cells on each film after 2 weeks of culture. (a) The flat film; (b) HC-PE; and (c) HC-CAP; the arrows indicate the fibroblastic cells.

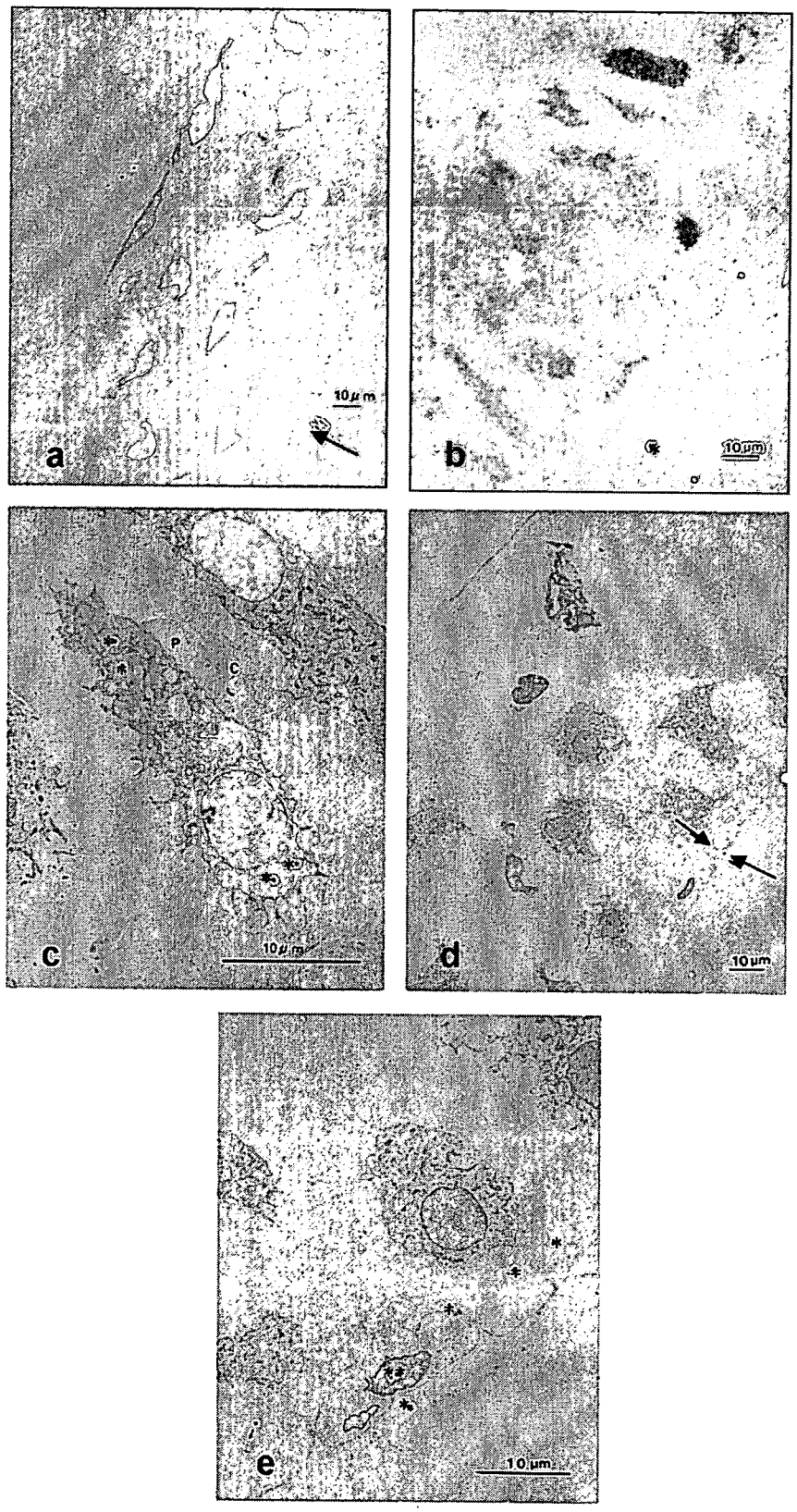

Fig. 5. TEM image of the chondrocytes cultured on each film after 2 weeks of culture. (a) The arrow indicates the flat film (1200×); (b) the asterisk indicate HC-PE (1600×); (c) P indicates cell vesicle; C indicates collagen; the asterisks indicate granular endoplasmic reticulum on HC-PE (6000×); (d) the arrows indicate HC-CAP (1600×) and (e) the asterisks indicate HC-CAP; the double asterisk indicates cells in the pore of the HC-CAP (4400×).

of culture. Cell proliferation was significantly higher on the flat film than on HC-PE ($p < 0.001$). It was clearly observed that cell proliferation was higher on HC-PE than that on HC-CAP ($p < 0.01$).

3.2. sGAG production

During culture, the chondrocytes produced ECM composed of sGAG. The sGAG analysis revealed that sGAG production, which was normalized by the DNA content, increased with time in the chondrocytes cultured on the flat film and HC-PE (Fig. 3). In the chondrocytes cultured on HC-CAP, sGAG production increased until 2 weeks and then leveled off at 3 weeks. Specifically, this increase in the sGAG production was consistently enhanced than that on other films ($p < 0.05$).

For the flat film and HC-PE, the number of the attached cells was proportional to the area of the film. The cell proliferation on each film was proportional to the DNA content, which illustrated the cell number. It is worthy of notice that sGAG production was not related to cell proliferation. Although the number of the cells on HC-PE was less than that on the flat film, all the chondrocytes present on HC-PE produced abundant sGAG. The chondrocytes exhibited a more extended morphology when growing on a two-dimensional surface, while a three-dimensional structure supported chondrocyte proliferation and differentiation [18]; this explains why the cells developed a more spherical morphology and produced abundant sGAG when growing on HC-PE. This implies that the topological property of the honeycomb-patterned film acts in a similar manner as that of a three-dimensional surface and affects the chondrocyte morphology.

3.3. Cell morphology

Toluidine blue-stained sections of the cultured cells showed the cell morphology and the distribution of ECM. Histological observation revealed that satisfactory chondrocyte proliferation and abundant matrix production surrounding each cell was visible on HC-PE (Fig. 4b). In contrast, the cells on the flat film appeared smaller and produced less ECM (Fig. 4a). The number of the cells present on HC-CAP was less than that on HC-PE (Fig. 4c). Some cells on the upper side exhibited a fibroblastic morphology (Fig. 4a–c).

On HC-PE, the TEM image revealed abundant ECM as well as good retention of the spherically differentiated chondrocyte morphology (Fig. 5b). Fig. 5c showed that the cells contained abundant rough endoplasmic reticulum, and the chondrocytes produced abundant collagen around themselves. Interestingly, the chondrocytes on HC-PE were orderly and columnar in appearance; on the contrary, those on HC-CAP were disorderly (Fig. 5d) with a smaller cell size. The cell size of the chondrocytes on the flat film was smaller than that of those on the honeycomb-patterned films, and the chondrocytes present on the surface displayed a flattened morphology (Fig. 5a). In addition, TEM analysis indicated that the chondrocytes migrated into the pores of the honeycomb-patterned film (Fig. 5e). They were flattened in a manner similar to that of a fibroblast and produced small amounts of ECM on the flat film. On the contrary, the chondrocytes cultured on the honeycomb-patterned films were observed to retain their spherical shape and produced abundant ECM. The results indicate that the honeycomb-patterned structure reduced the points of attachment for the chondrocytes, and possessed the potential to provide chondrocytes with a suitable environment for developing a spherical shape.

HC-PE demonstrated better results than HC-CAP with regard to all aspects probably due to the differences between the surfactants. HC-PE contained DOPE as a surfactant, which is a completely bioresorbable phospholipid with unsaturated fatty acid moieties. On the contrary, CAP is a synthetic polymer, which is synthesized from poly(acrylamide) derivatives, and its metabolic pathway in the body is yet to be clarified. From a point of view of safety, the HC-PE film is considerably more preferable as compared to the HC-CAP film because DOPE is a natural compound. Since for phospholipids are present in ECM, DOPE may have beneficial effects on the chondrocytes.

4. Conclusions

We reported that HC-PE had a strong influence on sGAG production and cell morphology, and that chondrocytes maintained their differentiated form when growing on HC-PE. In comparison, the chondrocytes on the flat film exhibited high cell proliferation but sGAG production was at a lower level, and the cells were not healthy. Based on these results, HC-PE displays potential as a scaffold for cartilage tissue engineering. However, further work is necessary in order to investigate for questions such as optimal pore size on film, chondrocyte phenotype retention, and in vivo behavior of the cells implant.

Acknowledgements

The authors thank Dr. Haruko Hirose of the Institute for Structure Analysis, Teijin Limited, for OM and TEM analysis and helpful discussions, Masato Ito for his kind help and advice, and Takami Hayashi for providing technical assistance in chondrocyte culture.

References

[1] P. Clark, S. Britland, P. Connolly, Growth cone guidance and neuron morphology on micropatterned laminin surfaces, J. Cell Sci. 105 (1993) 203.
[2] Y. Xia, G.M. Whitesides, Soft lithigraphy, Angew. Chem. Int. Ed. 37 (1998) 550.
[3] H. Lo, S. Kadiyala, S.E. Guggino, K.W. Leong, Poly(L-lactic acid) foams with cell seeding and controlled-release capacity, J. Biomed. Mater. Res. 30 (1996) 475.
[4] S. Sedrakyan, Z. Zhou, L. Perin, K. Leach, D. Mooney, T. Kim, Tissue engineering of a small hand phalanx with a porously casted polylactic acid-polyglycolic acid copolymer, Tissue Eng. 12 (2006) 2675.
[5] B. Wang, T. He, L. Liu, C. Gao, Poly(ethylene glycol) micro-patterns as environmentally sensitive template for selective or non-selective adsorption, Colloids Surf. B 46 (2005) 169.
[6] M. Shimomura, T. Sawadaishi, Bottom-up strategy of materials fabrication: a new trend in nanotechnology of soft materials, Curr. Opin. Colloid Interface Sci. 6 (2001) 11.